Terrestrial CO_2 fluxes, concentrations, and budgets in USA and Northeast China

Xiao-Ming Hu[1], and Xiaolan Li[2]

http://www.caps.ou.edu/~xhu/

2019-06-20 @ Institute of Subtropical Agriculture, Chinese Academy of Sciences

[1]Center for Analysis and Prediction of Storms,and School of Meteorology, University of Oklahoma
[2]Institute of Atmospheric Environment, China Meteorological Administration, Shenyang

CO_2-induced global warming?

Trend of CO_2

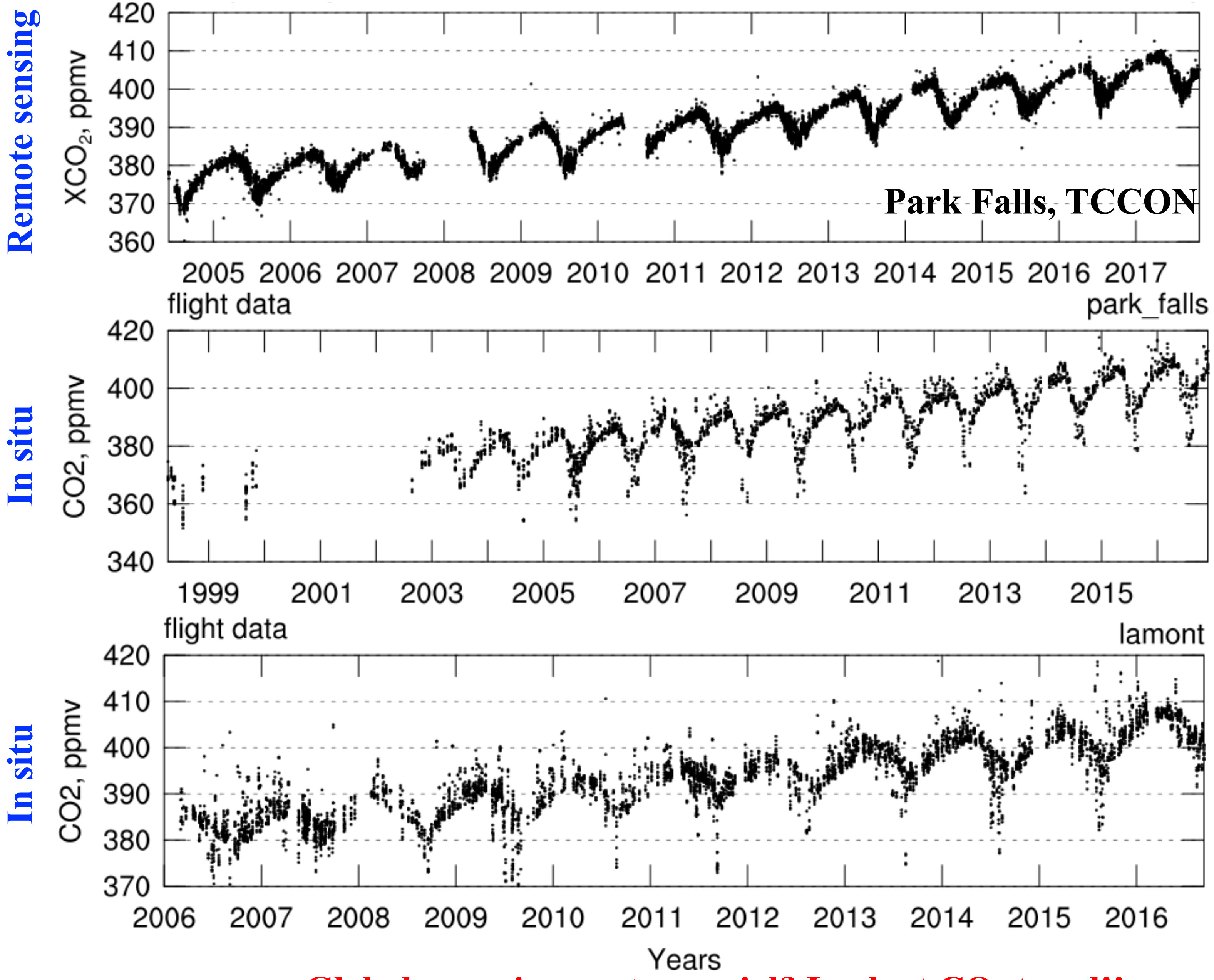

Global warming controversial? Look at CO_2 trend!!

Global CO_2 sources and sinks

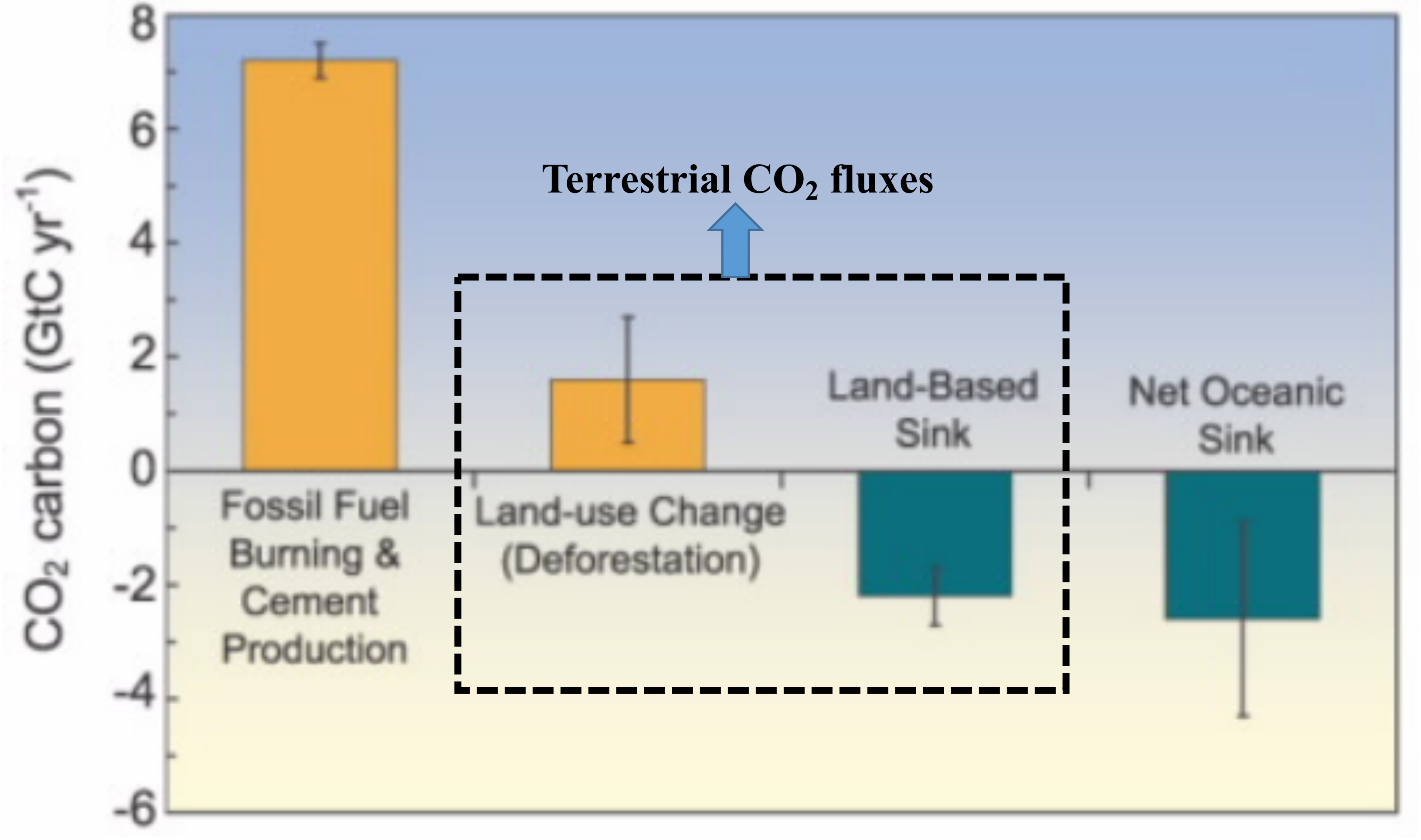

IPCC (2007)

Uncertainties of terrestrial CO_2 fluxes are large

Terrestrial CO_2 fluxes in different regions

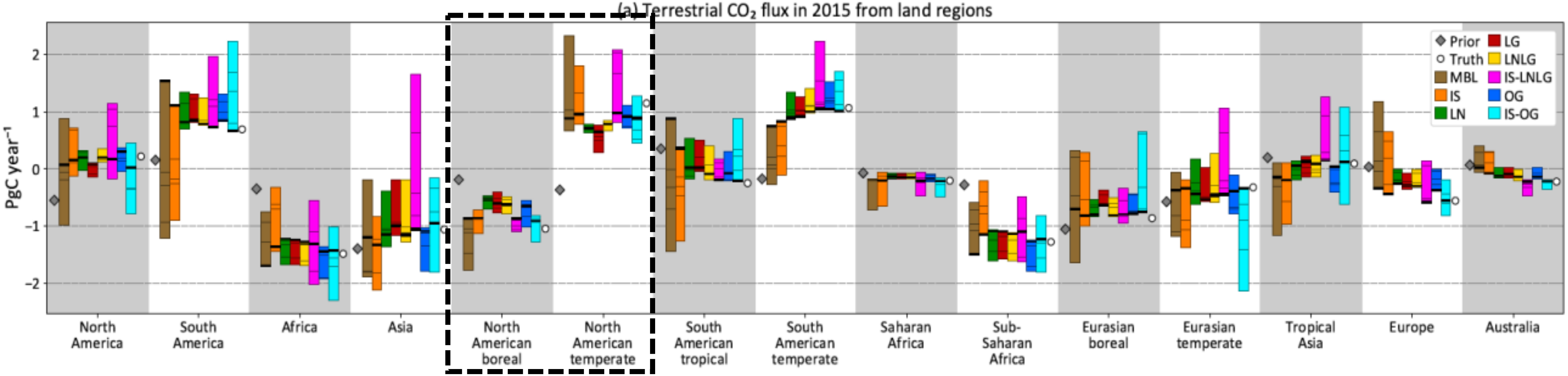

(Sourish Basu et al., 2018)

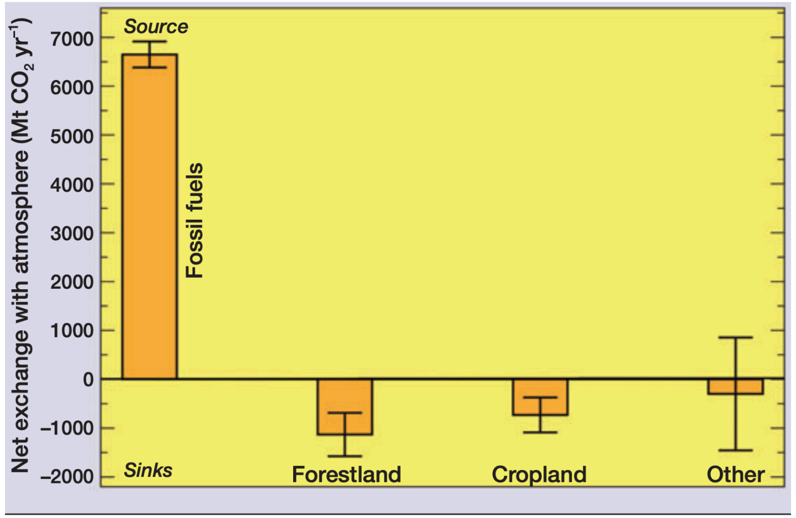

King et al., 2012 *North American CO_2 sources and sinks, circa 2010. The fossi*

Uncertainties in each region/plant function are large too

WRF/Chem-VPRM for CO_2 simulation

- Vegetation Photosynthesis and Respiration Model (VPRM) (Xiao et al., 2004; Mahadevan et al., 2008; Ahmadov et al., 2007)

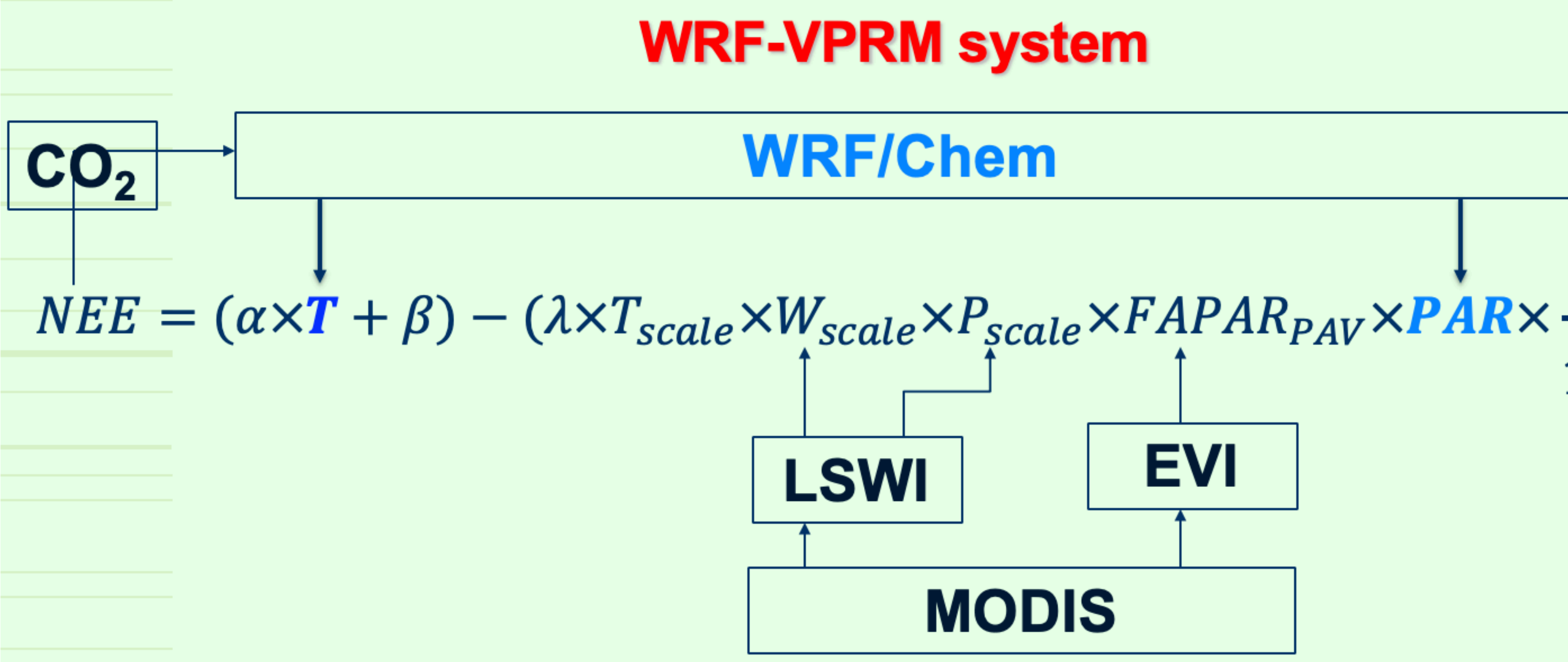

$$NEE = (\alpha \times T + \beta) - \left(\lambda \times T_{scale} \times W_{scale} \times P_{scale} \times FAPAR_{PAV} \times PAR \times \frac{1}{1 + \frac{PAR}{PAR_0}}\right)$$

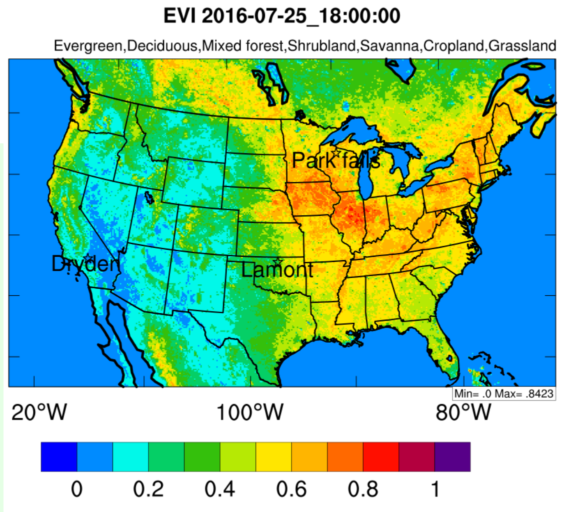

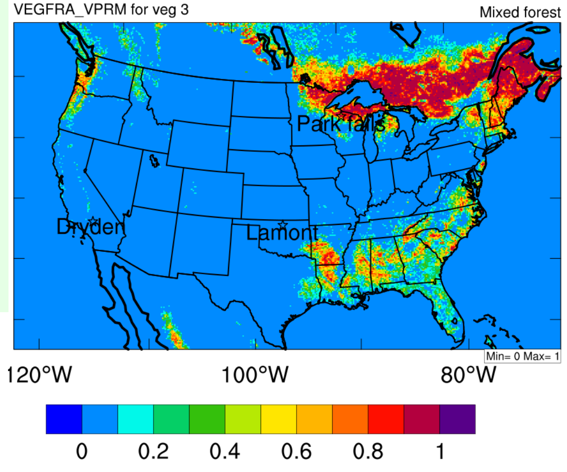

Implemented parameters from Hilton, Davis et al. (2013)

Calibrated using eddy covariance tower data over North America

	Evergreen forest	Deciduous forest	Mixed forest	Shrub	Savanna	Crop	Grass
PAR_0	745.306	514.13	419.5	590.7	600	1074.9	717.1
λ	0.13	0.1	0.1	0.18	0.18	0.085	0.115
α	0.1247	0.092	0.2	0.0634	0.2	0.13	0.0515
β	0.2496	0.843	0.27248	0.2684	0.3376	0.542	-0.0986

And other minor changes to VPRM in WRF

Downscaling in year 2016 from CT-NRT.v2017

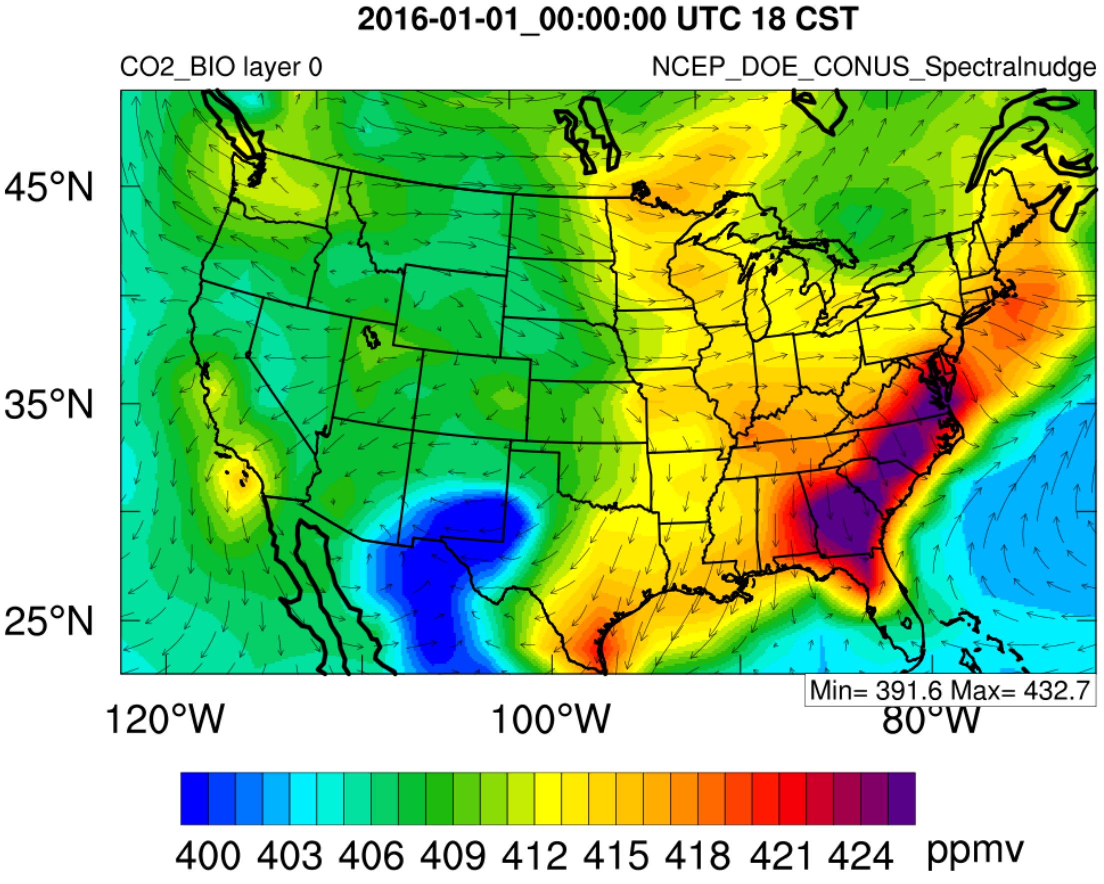

WRF-VPRM IC

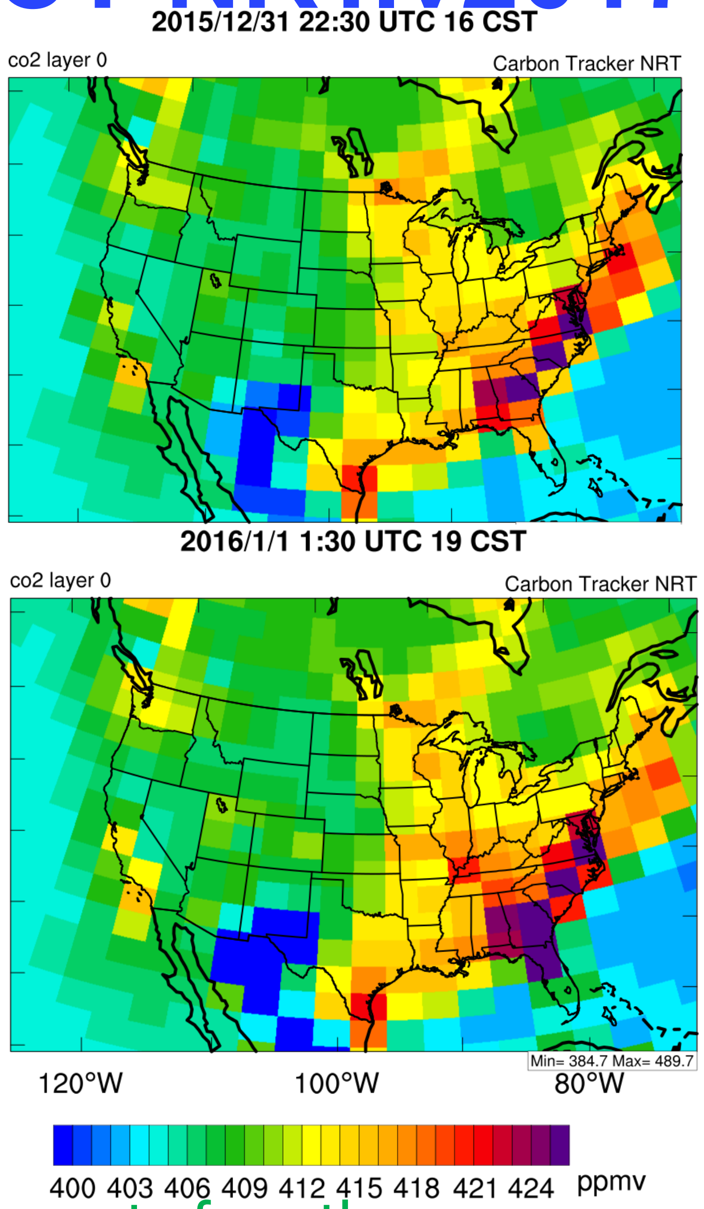

Point 1: both IC/BC are time dependent

Point 2: resolution of WRF-VPRM is much higher, adequate to investigate impact of weather

configuration for WRF-VPRM downscaling

Short wave radiation	Dudhia
Long wave radiation	rapid radiative transfer model (RRTM)
Boundary layer	YSU
Microphysics	Morrison
Cumulus	Grell-Freitas
Land surface model	NOAH
Vertical levels	47
Horizontal resolution	12 km $\times$ 12 km with 266$\times$443 grid points
Time step	60 seconds
Meteo initial and lateral boundary conditions	NCEP/DOE Reanalysis 2 (R2)
CO_2 initial and lateral boundary conditions	**CarbonTracker** global simulation $3^o \times 2^o$ outputs
Interior nudging	**Spectral nudging**
nudging variables	horizontal wind components, temperature, geopotential
nudging coefficient	3×10^{-5} s^{-1}
nudging height	above PBL
wave number	5 and 3 in the zonal and meridional directions respectively
nudging period	throughout the downscaling simulation

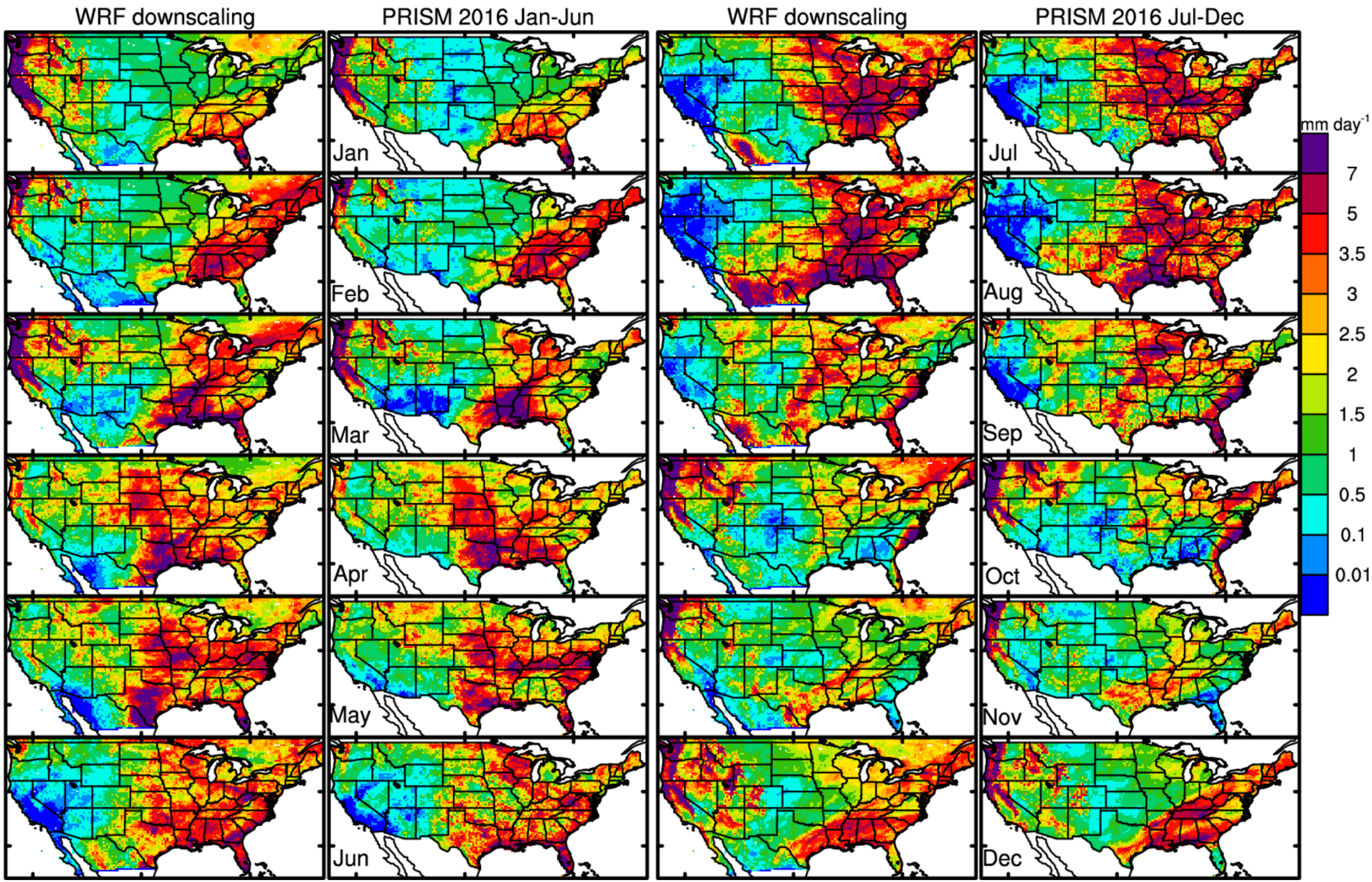

Downscaling captures the monthly variation of precipitation

Biogenic CO_2 fluxes downscaled by WRF-VPRM vs. CarbonTracker posterior fluxes

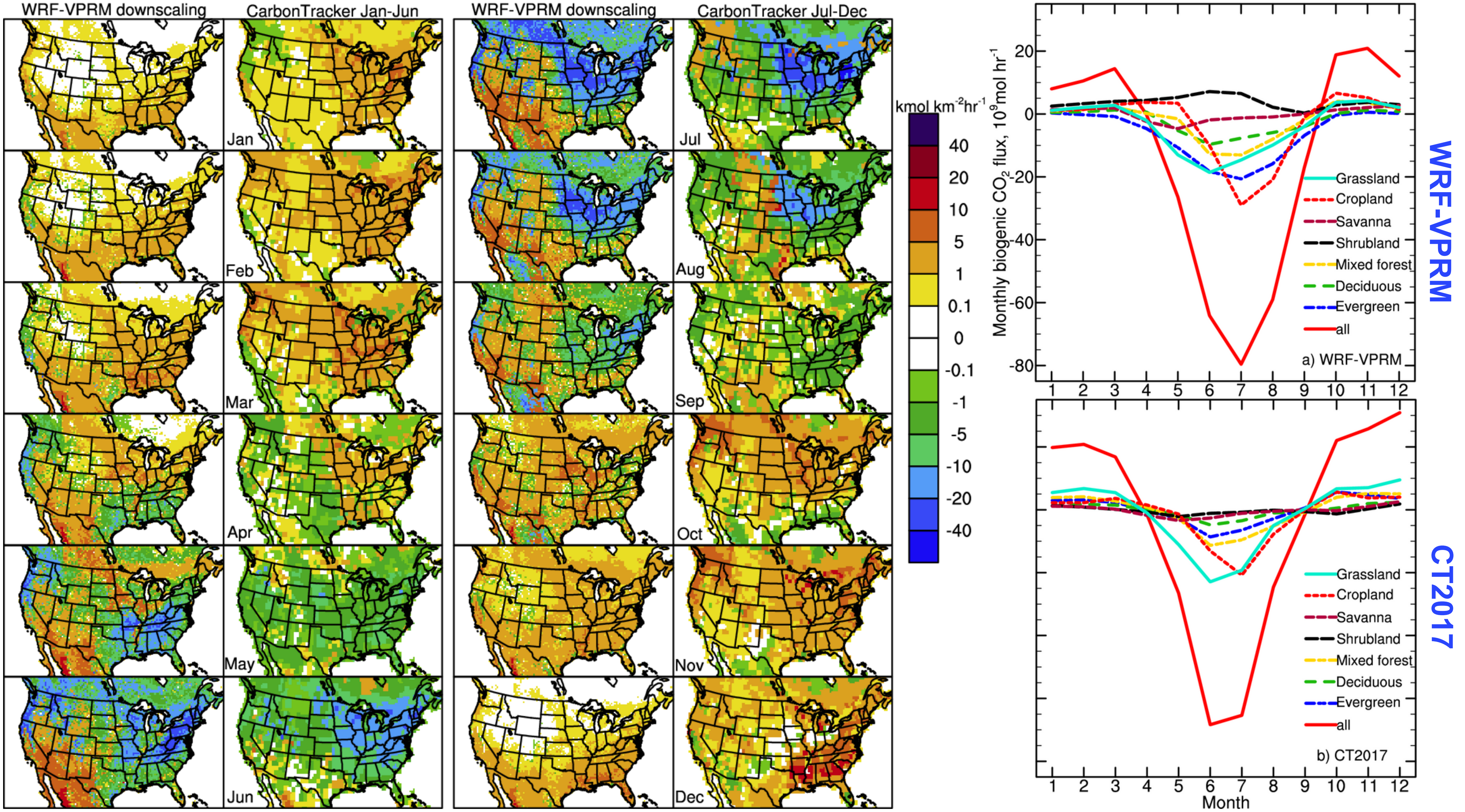

XCO_2 at the 4 TCCON sites

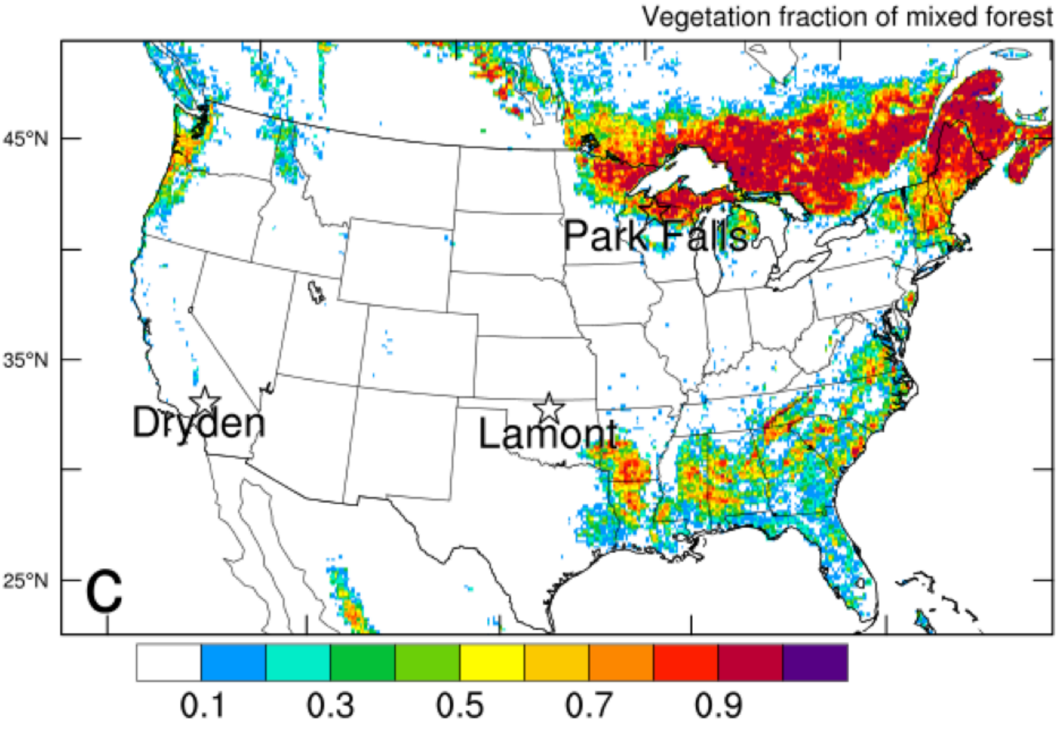

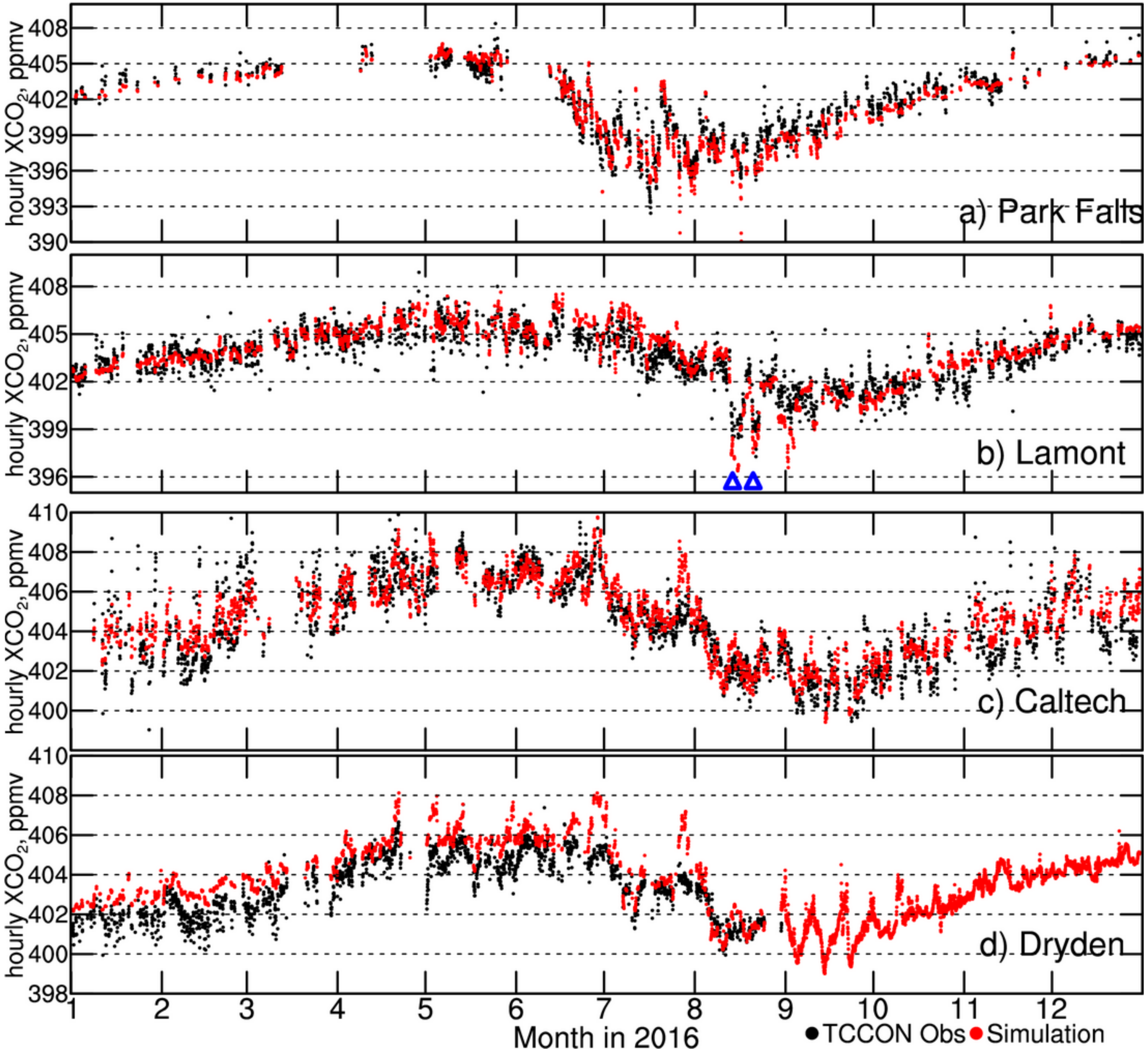

Bias in western boundary?
Bias in anthropogenic emission?

captures the seasonal and some episodic variation of XCO_2.

Evaluation of CT2017

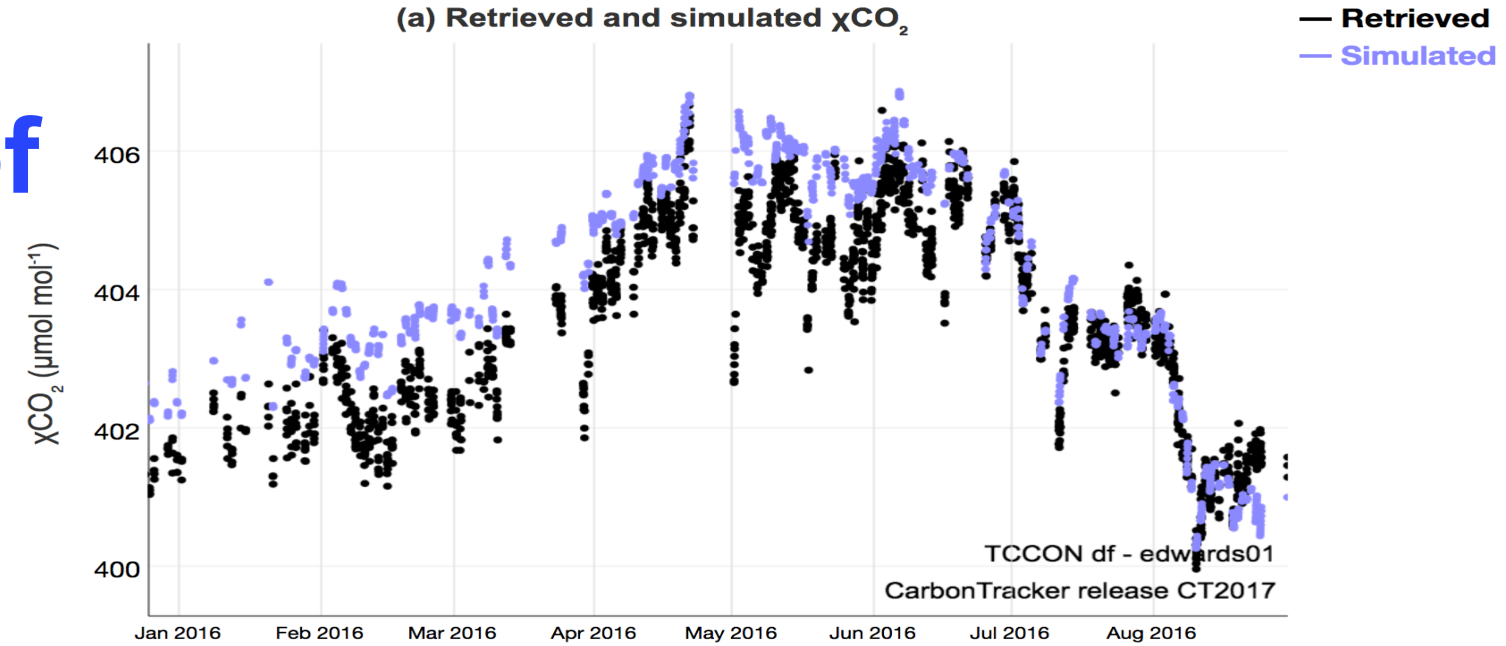

Evaluation of WRF-VPRM

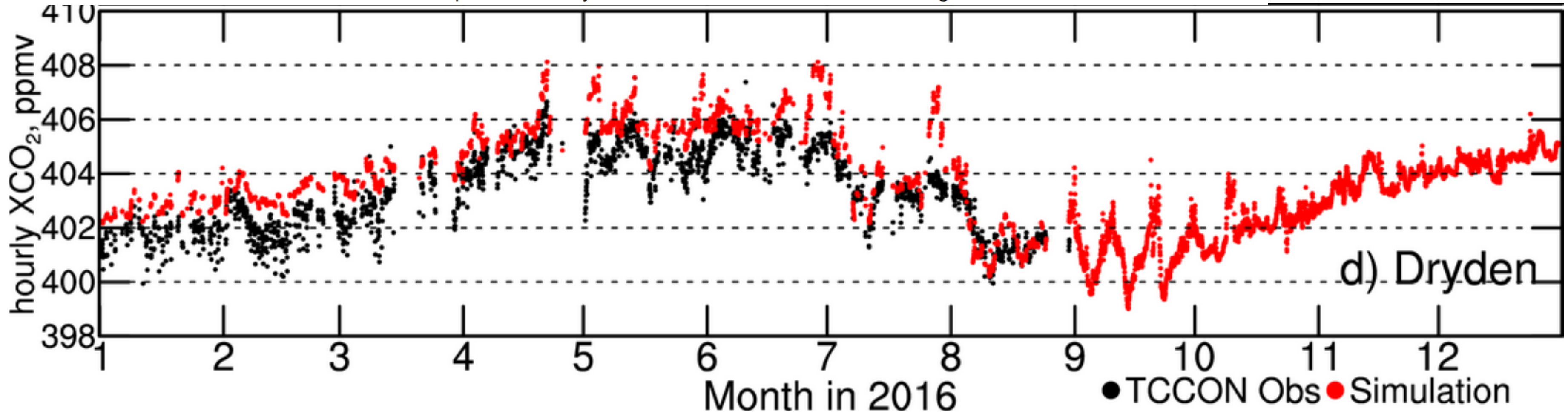

Thus, bias in western boundary partially contributed to WRF-VPRM bias?

Individual contribution to XCO_2

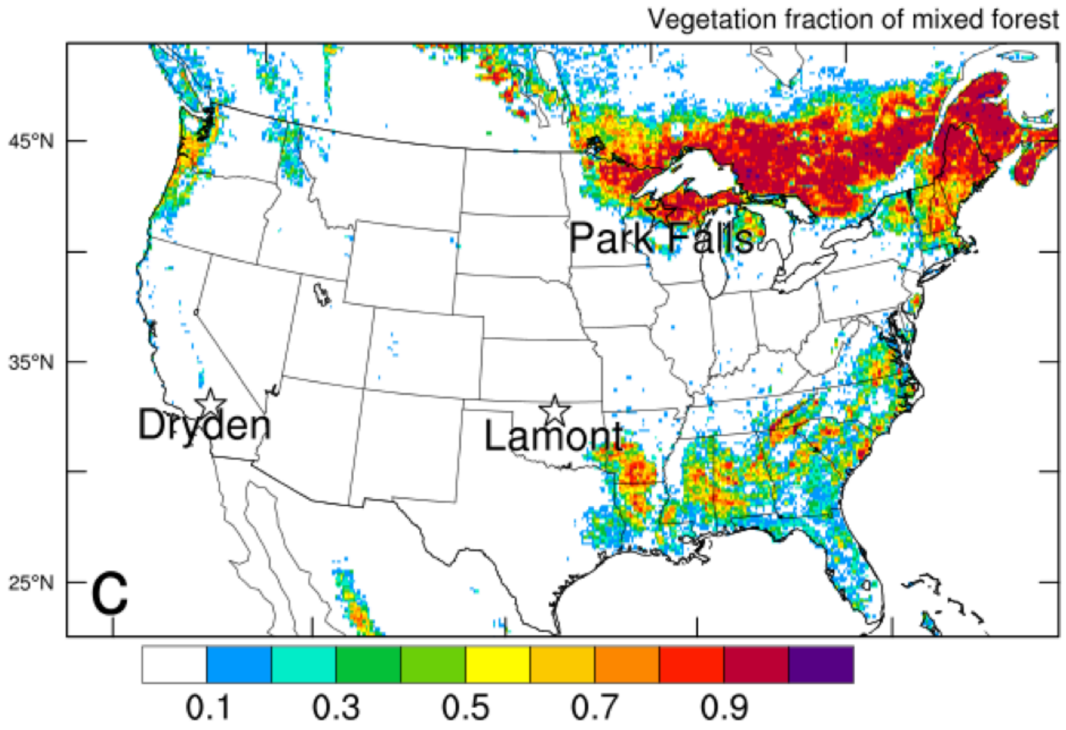

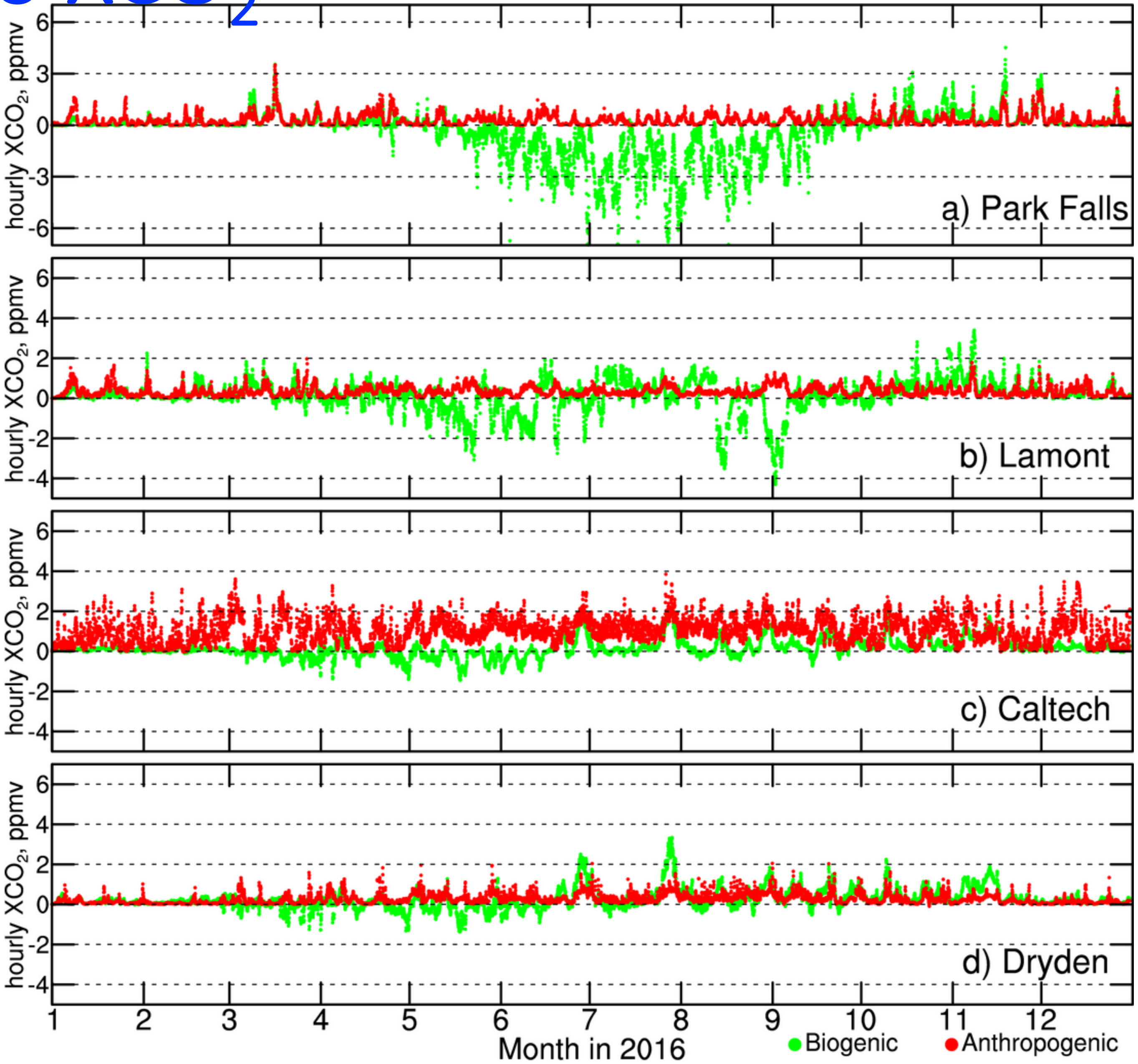

Compare with OCO-2; individual contributions

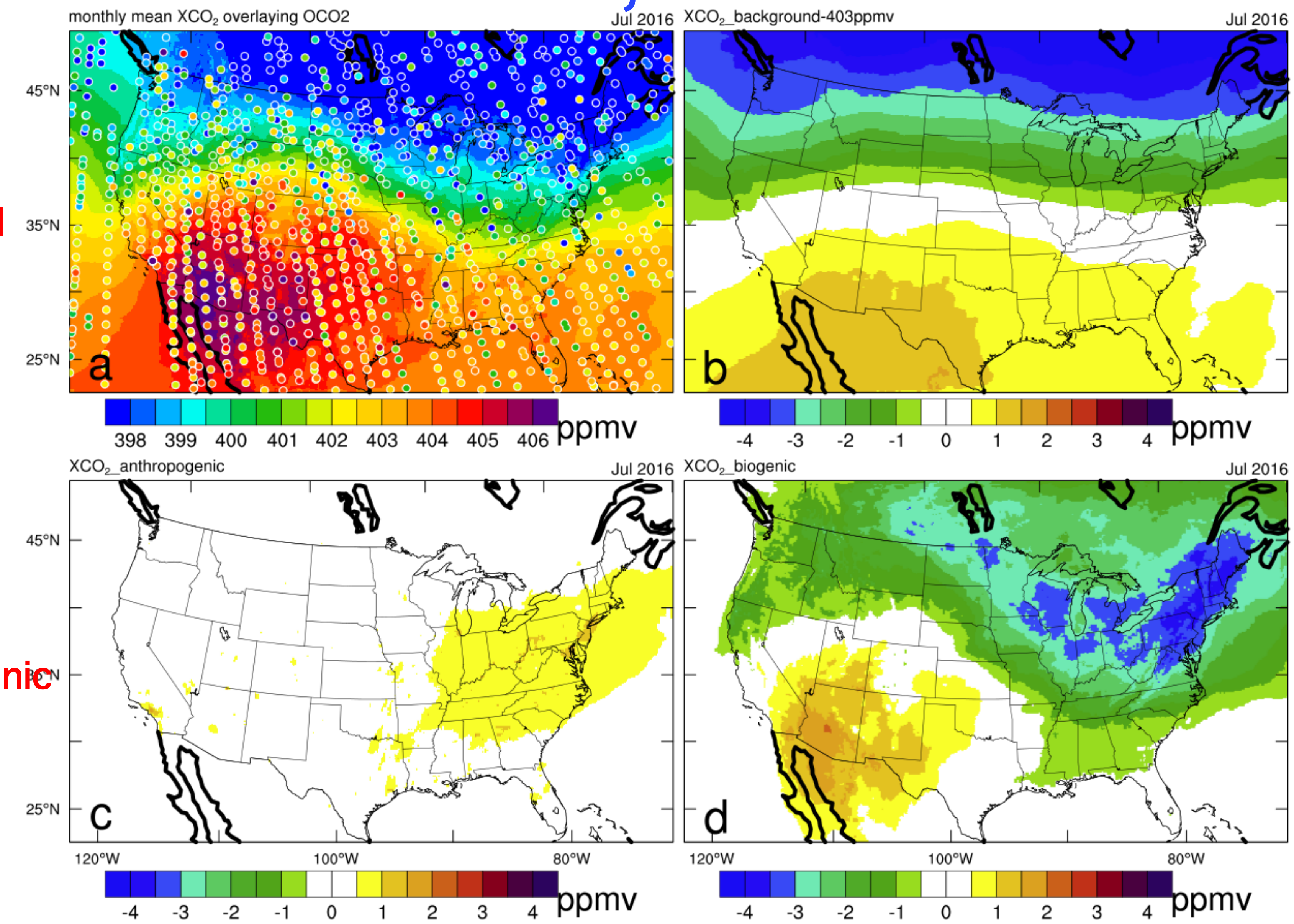

Total

Background

Anthropogenic

Biogenic

Compare with OCO-2, individual cases

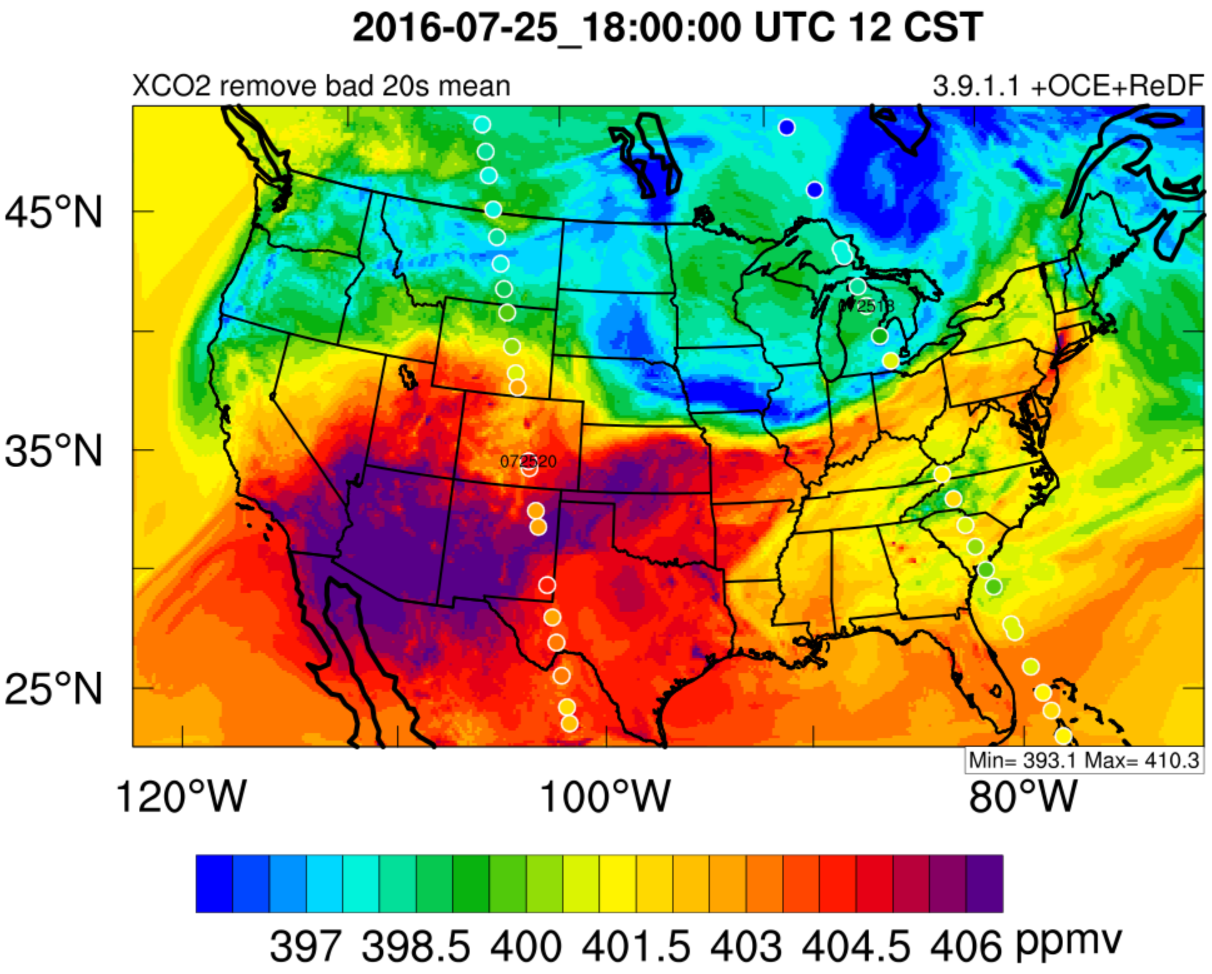

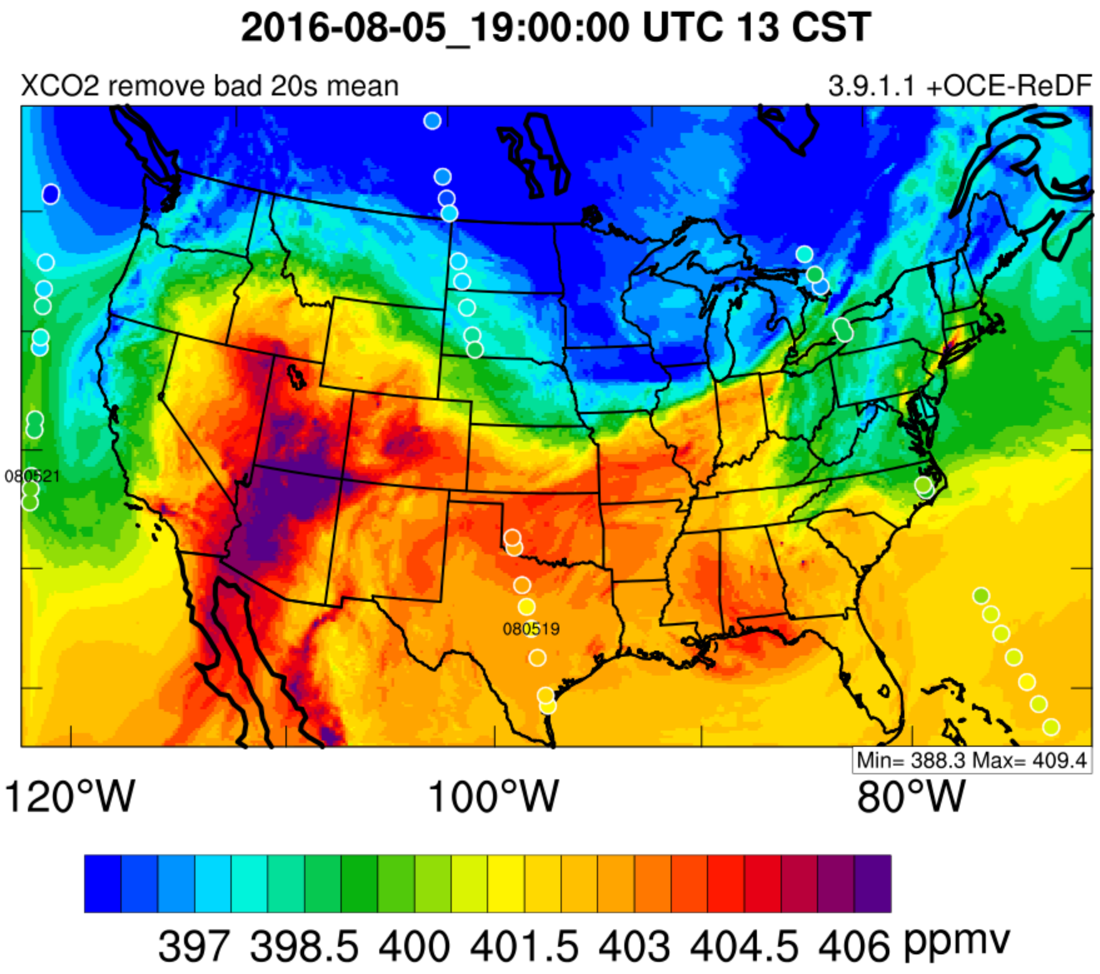

Statistic evaluation of XCO_2 using OCO-2 data

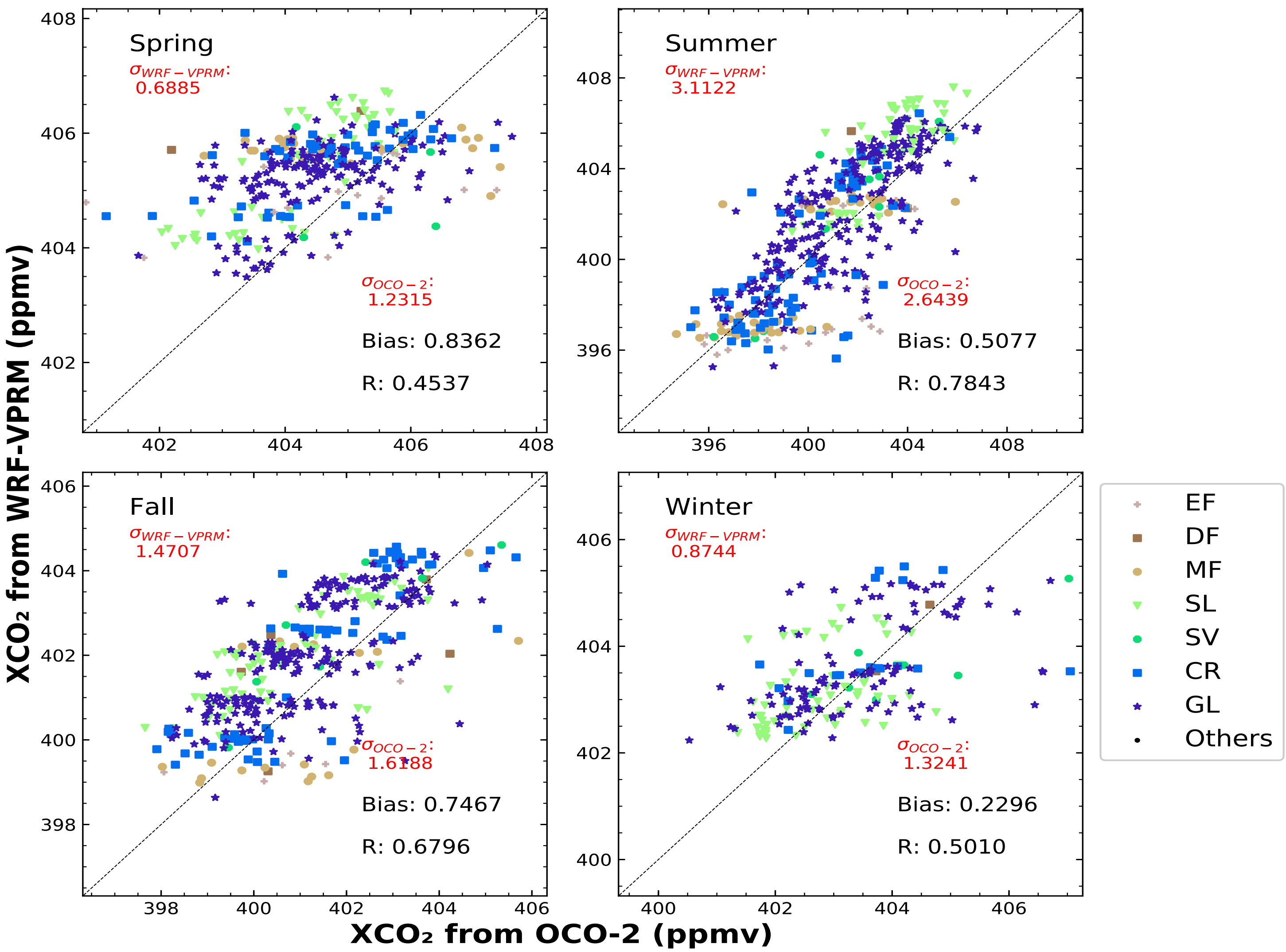

Best performance in Summer, followed by Fall

Case study
July 25

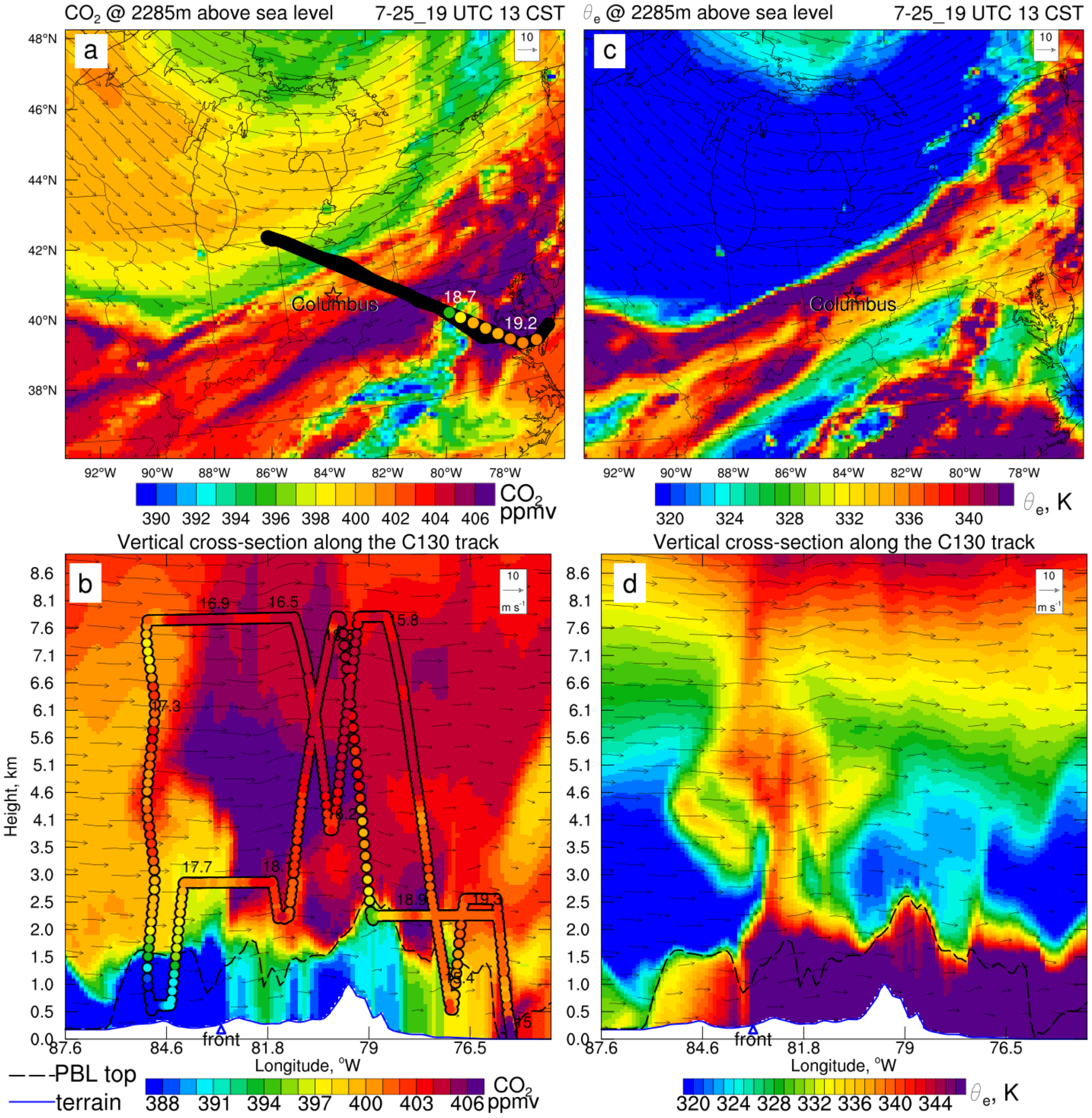

Capture the contrast across boundary layer top

Case study, Aug 5
OCO-2 underpass

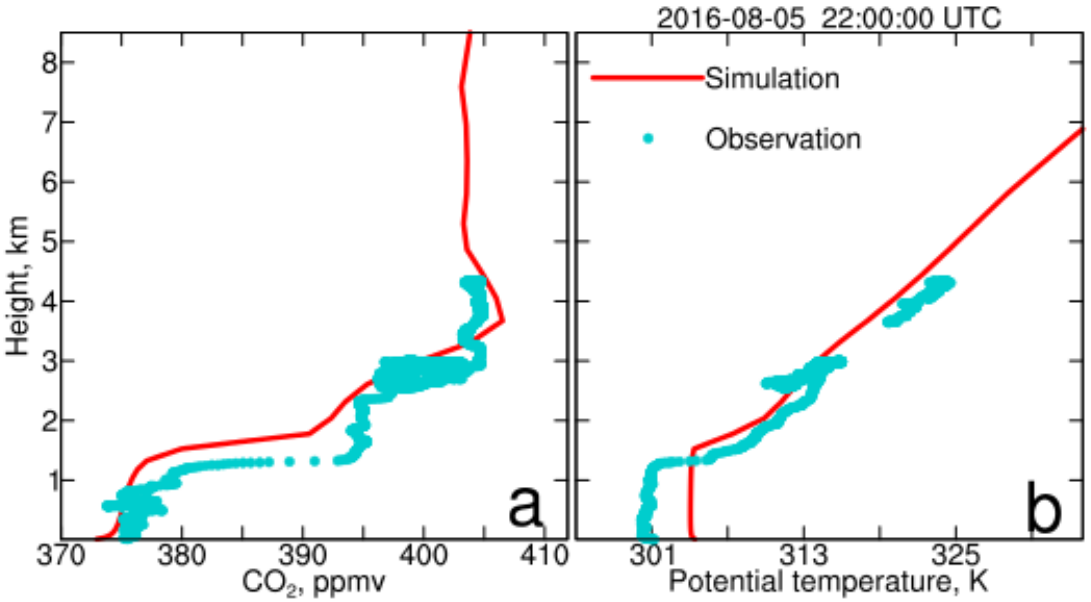

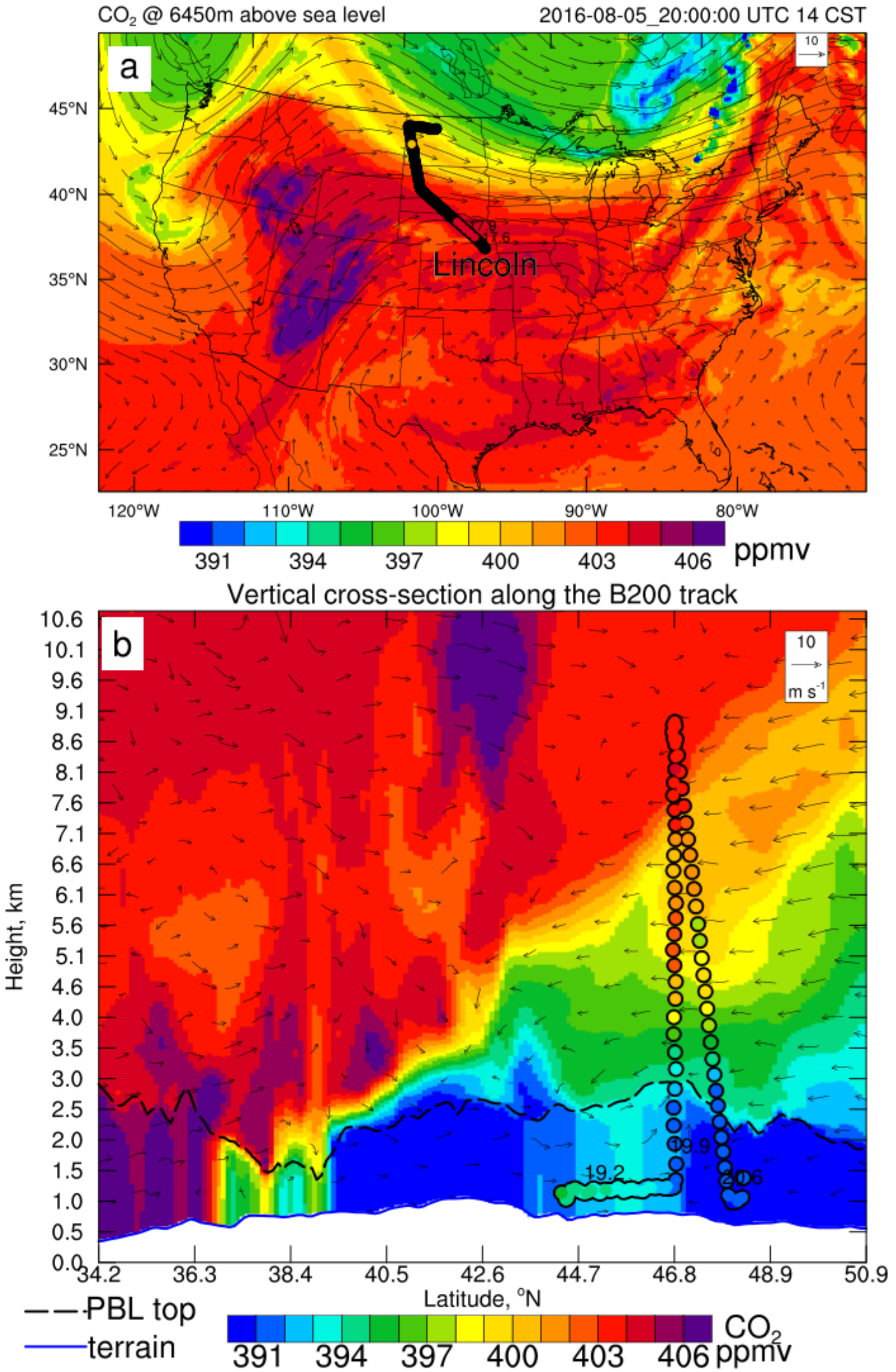

Aug 21,2016

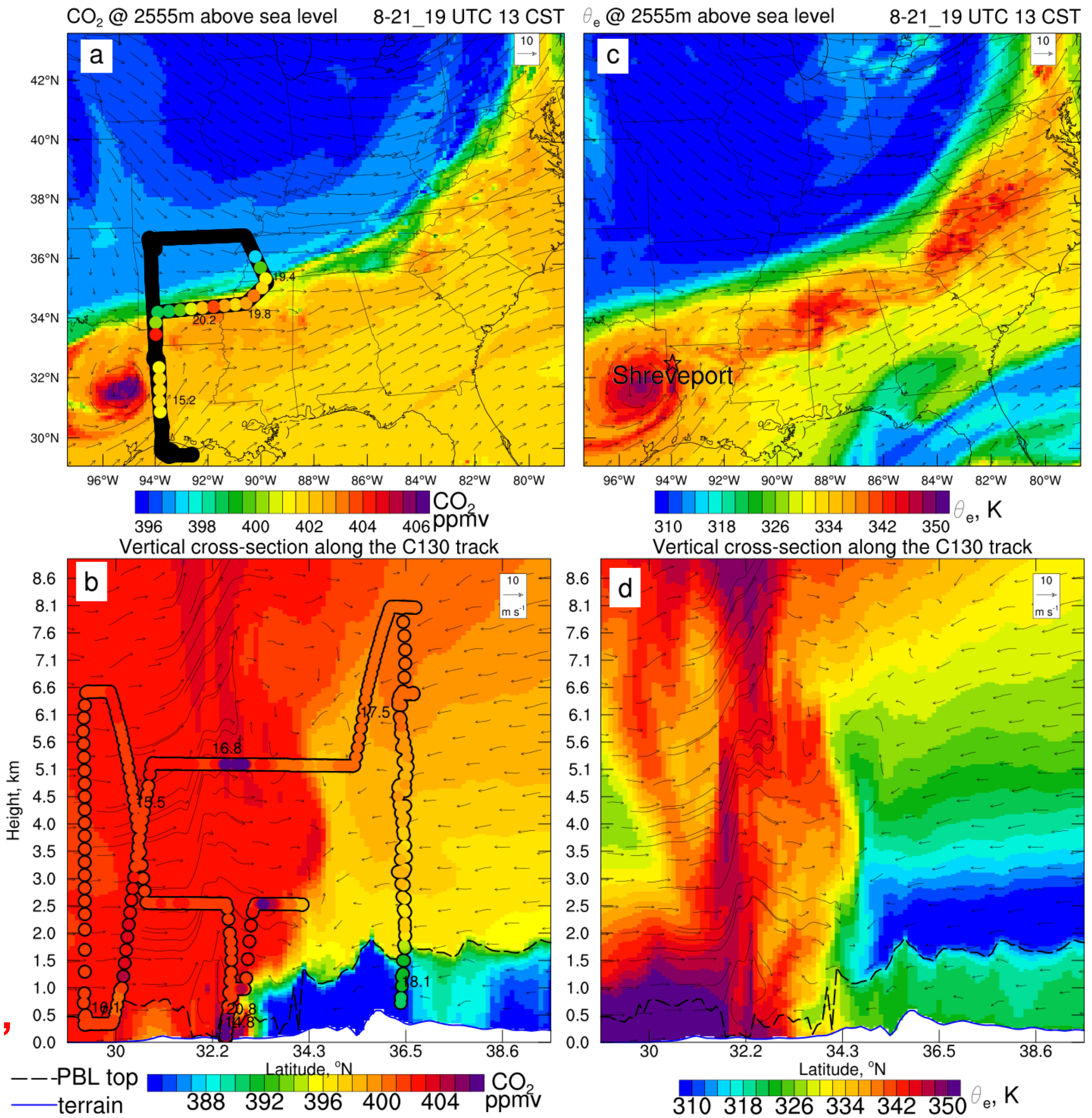

Capture the contrast across boundary layer top, and across cold front

Summary

1. Calibrated VPRM parameters from Hilton et al [2013] are implemented into WRF-VPRM
2. WRF-VPRM reasonably captures monthly variation of XCO_2 and episodic variations due to frontal passages
3. The downscaling also successfully captures the horizontal CO_2 gradients across fronts, as well as vertical CO_2 contrast across the boundary layer top.

Terrestrial CO_2 fluxes in different regions

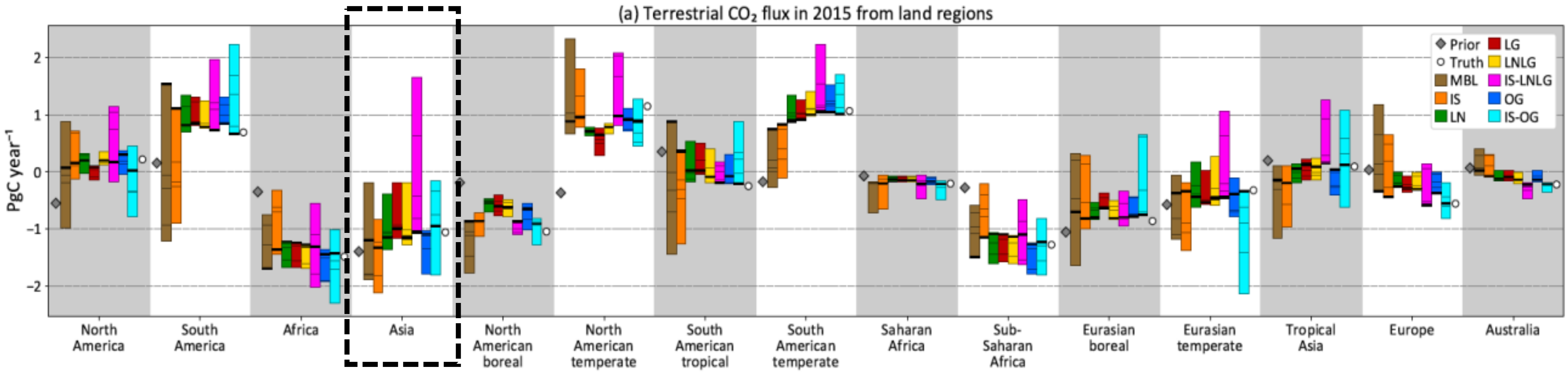

(Sourish Basu et al., 2018)

Uncertainties in each region are large too

Asia is CO_2 sink!!

Northeast China: a major CO_2 sink

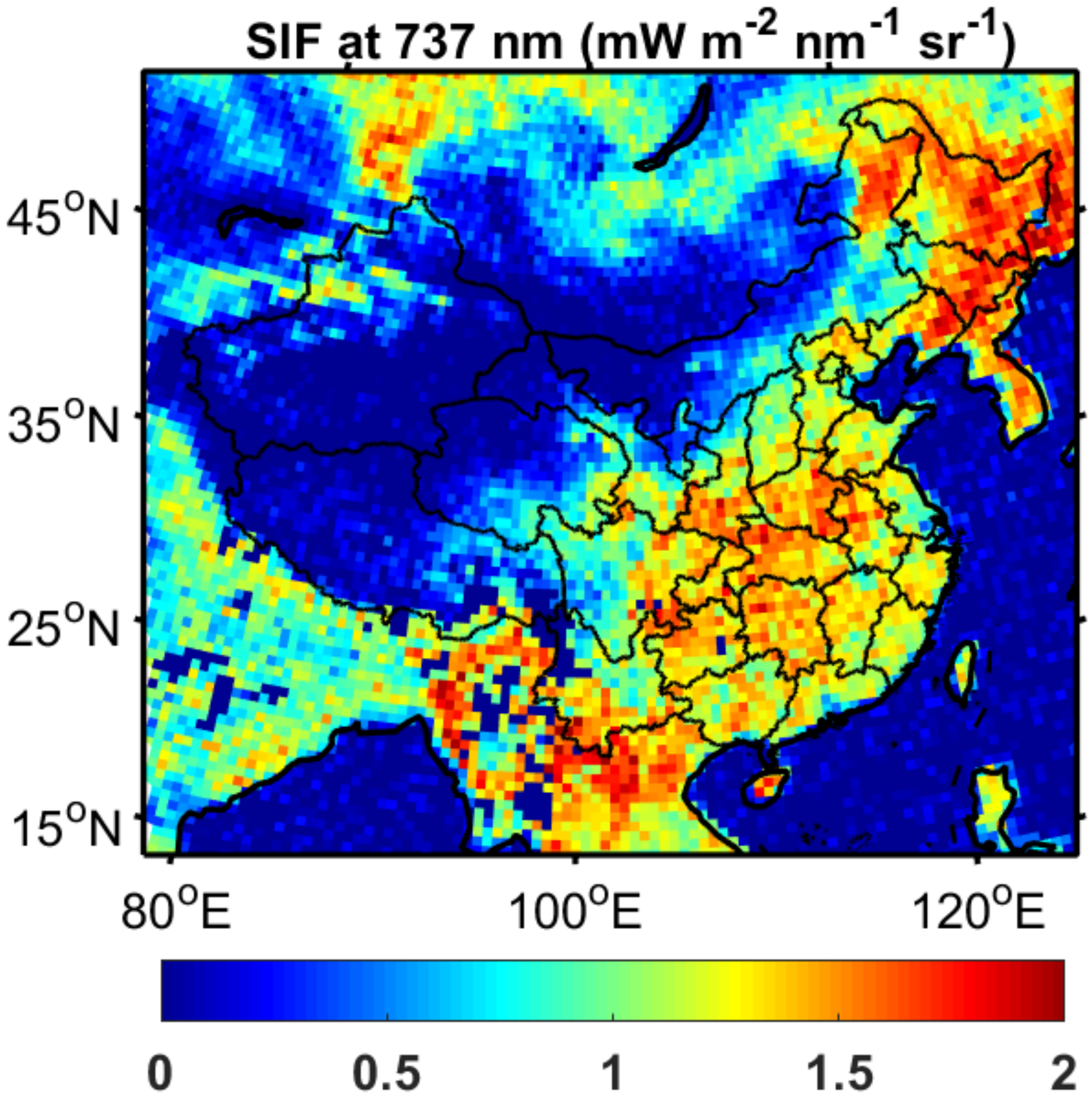

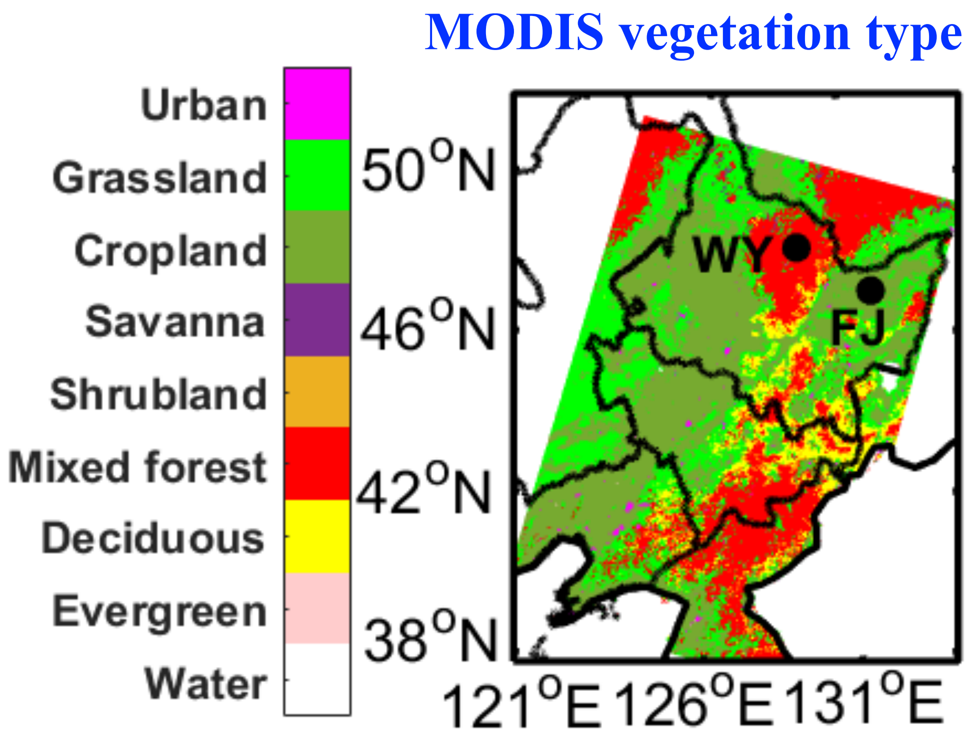

Mixed forest and cropland dominate in Northeast China

Crop area is still increasing!!

SIF: Sun-induced Fluorescence, proportional to photosynthesis

Long-term tower measurements, focusing on 2016

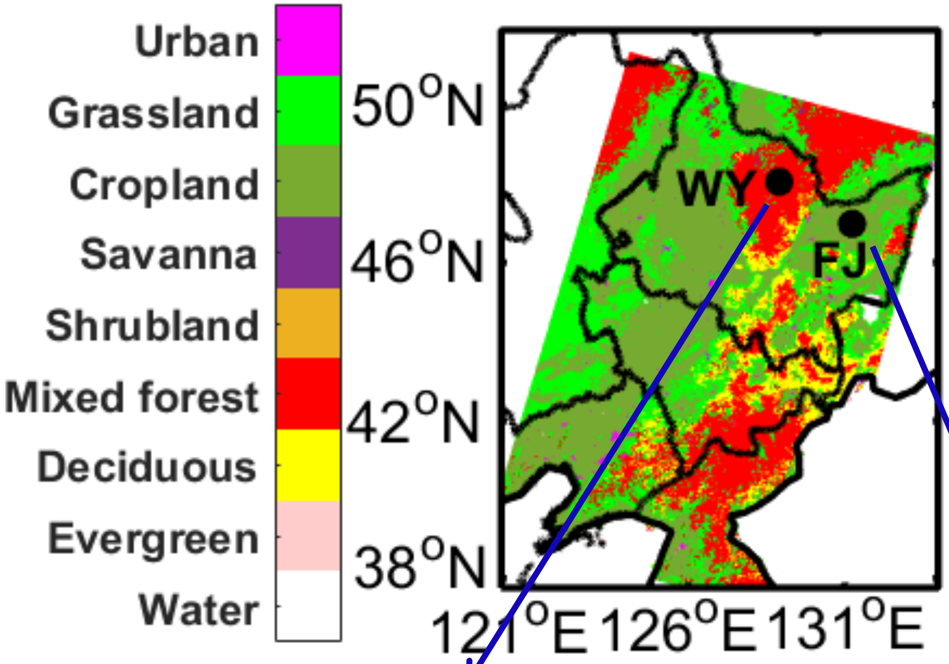

- **Observational parameters:**
  1) Hourly mean CO_2 fluxes and concentrations,
  2) wind speed and direction, air temperature
  3) PAR (only at Fujin)

- **Observational period:**
  Fujin: since 2012
  Wuying: since 2014


Wuying, mixed forest site
(131.9385° E, 47.1519° N, 345 m)

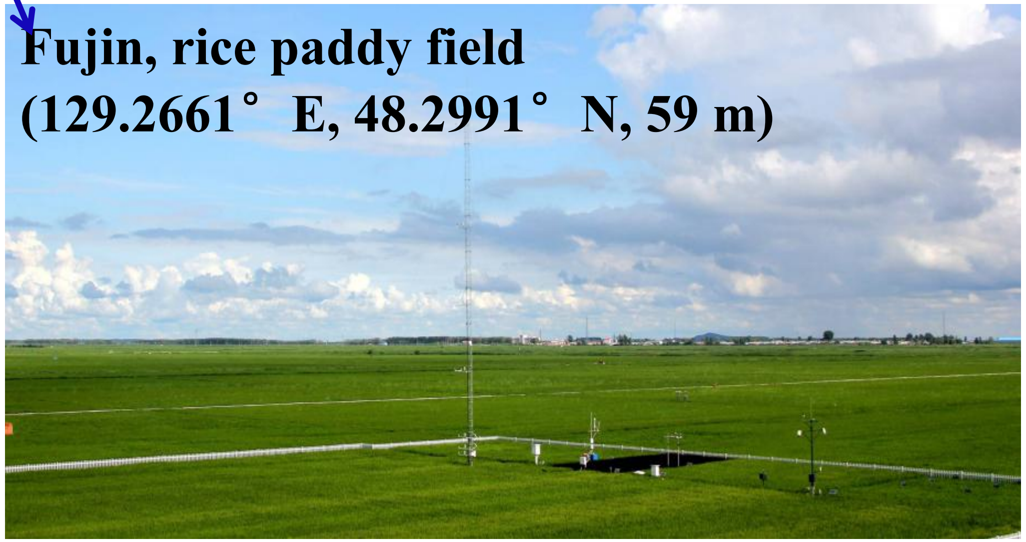
Fujin, rice paddy field
(129.2661° E, 48.2991° N, 59 m)

2016 downscaling using WRF-VPRM: a weather-biosphere-online-coupled model

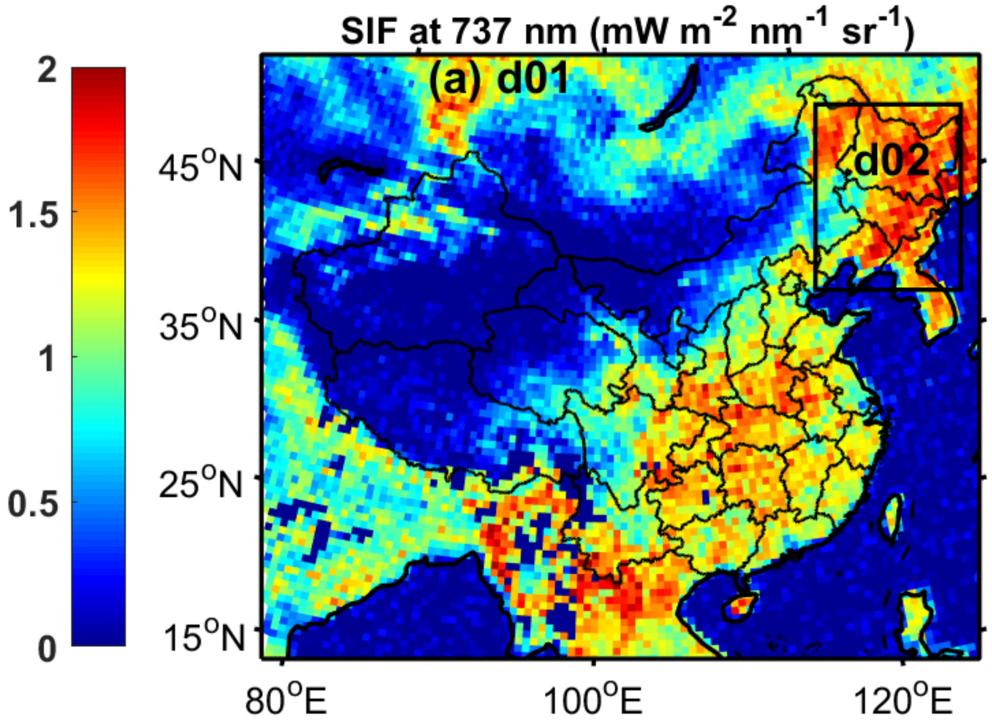

- **Resolution:** 20 km in d01; 4 km in d02
- **Meteorology initial/boundary conditions:** NECP/DOE R2
- **CO_2 initial/boundary conditions:** 3°×2° CarbanTracker 2017
- **Anthropogenic emissions of CO_2:** ODIAC

$$NEE = (\alpha \times T + \beta) + GEE$$

$$GEE = -\lambda \times T_{scale} \times W_{scale} \times P_{scale} \times \frac{1}{1+\frac{PAR}{PAR_0}} \times FAPAR_{PAV} \times PAR$$

maximum light use efficiency

water stress scale

phenology scale

photosynthetically active radiation

Related to land surface water index (LSWI)

Roughly equal to enhanced vegetation index (EVI)

	Crops	Mixed forest	Evergreen forest	Deciduous forest	Shrub	Savanna	Grass
α	0.1300	0.2000	0.1247	0.0920	0.0634	0.2000	0.0515
β	0.5420	0.27248	0.2496	0.8430	0.2684	0.3376	-0.0986
λ	0.085	0.100	0.130	0.100	0.180	0.180	0.115
PAR_0	1074.9	419.50	745.306	514.13	590.7	600.0	717.1

Following Hu et al. (2019) based on Hilton et al. (2013)

OCO-2 retrieved XCO_2 (L2 Lite Version 9)

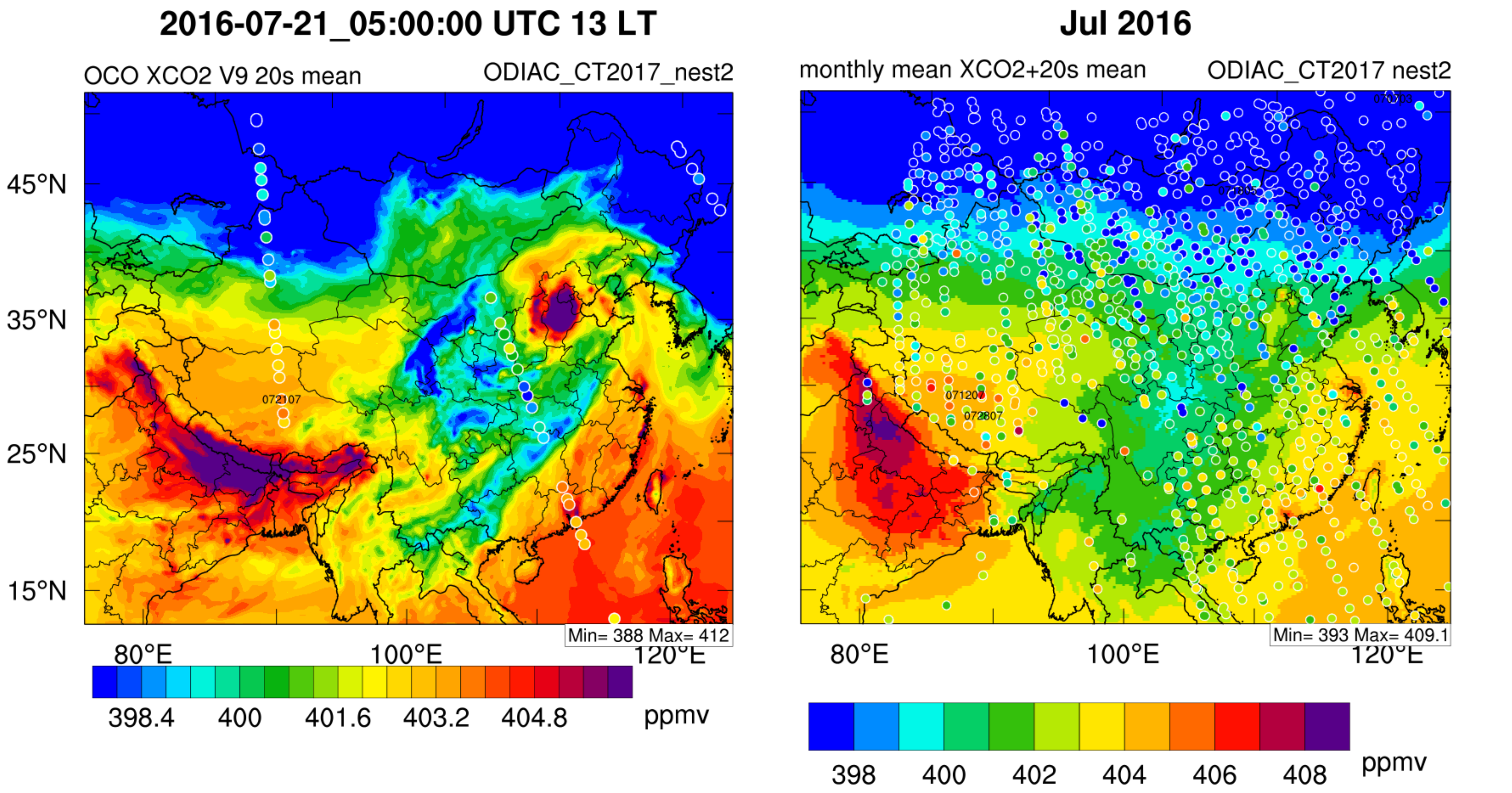

Advantage: spatiotemporal coverage

Disadvantage: interfere with cloud and haze pollution!!

Seasonal variations of CO_2 fluxes and concentrations

Fujin (cropland, rice paddy)

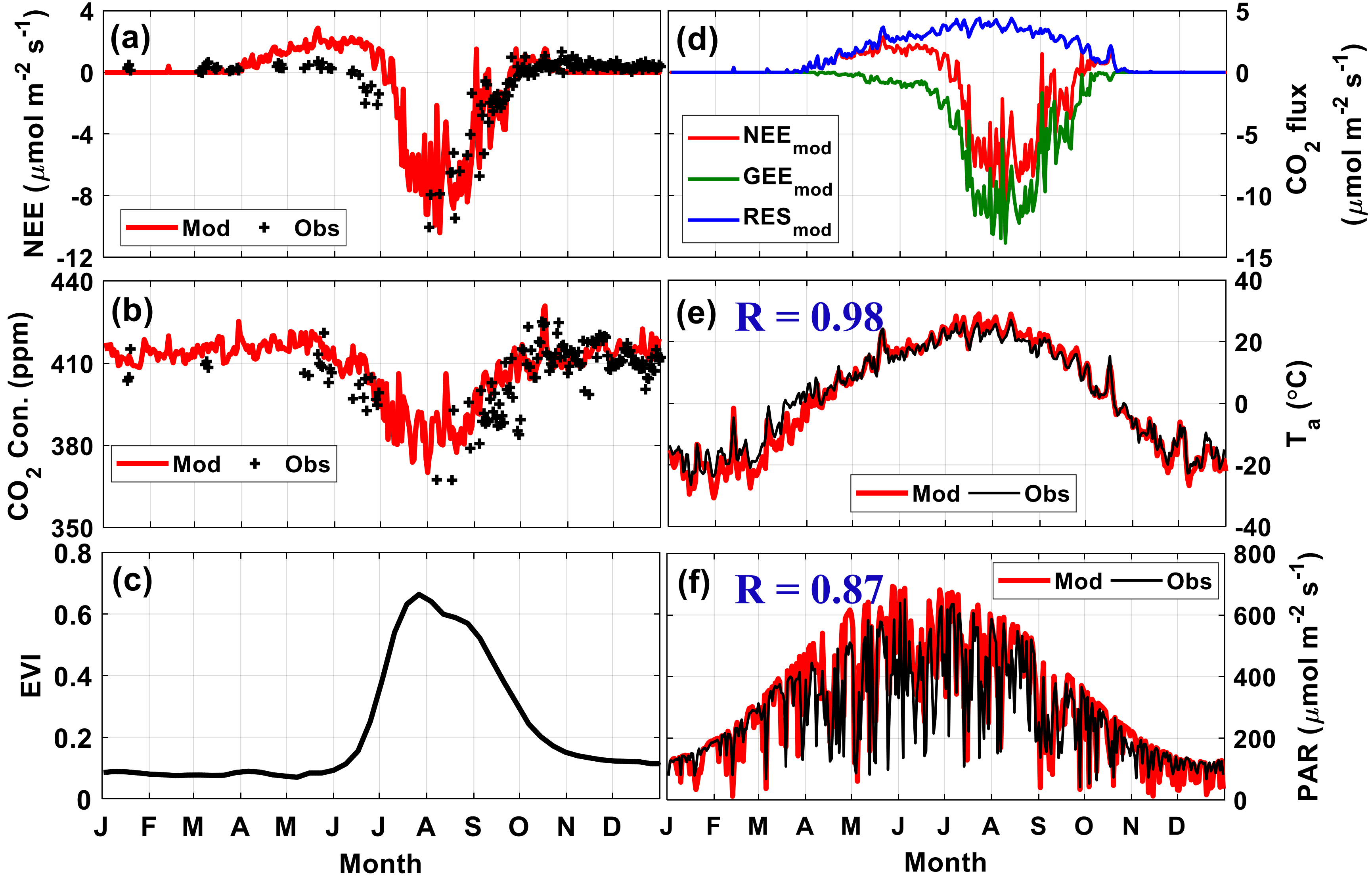

MODIS vegetation type

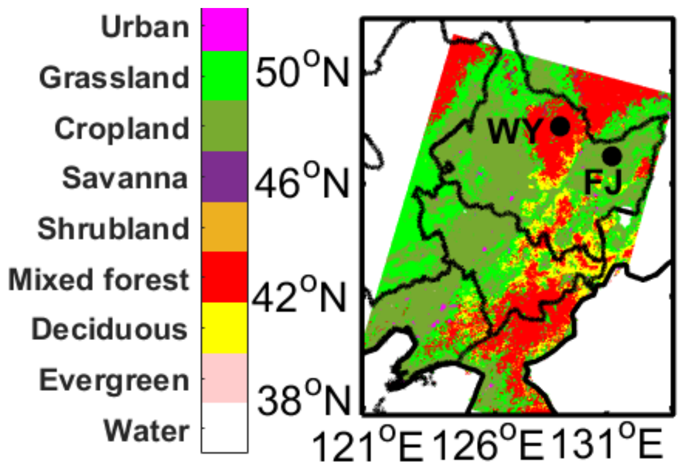

Bias of terrestrial respiration

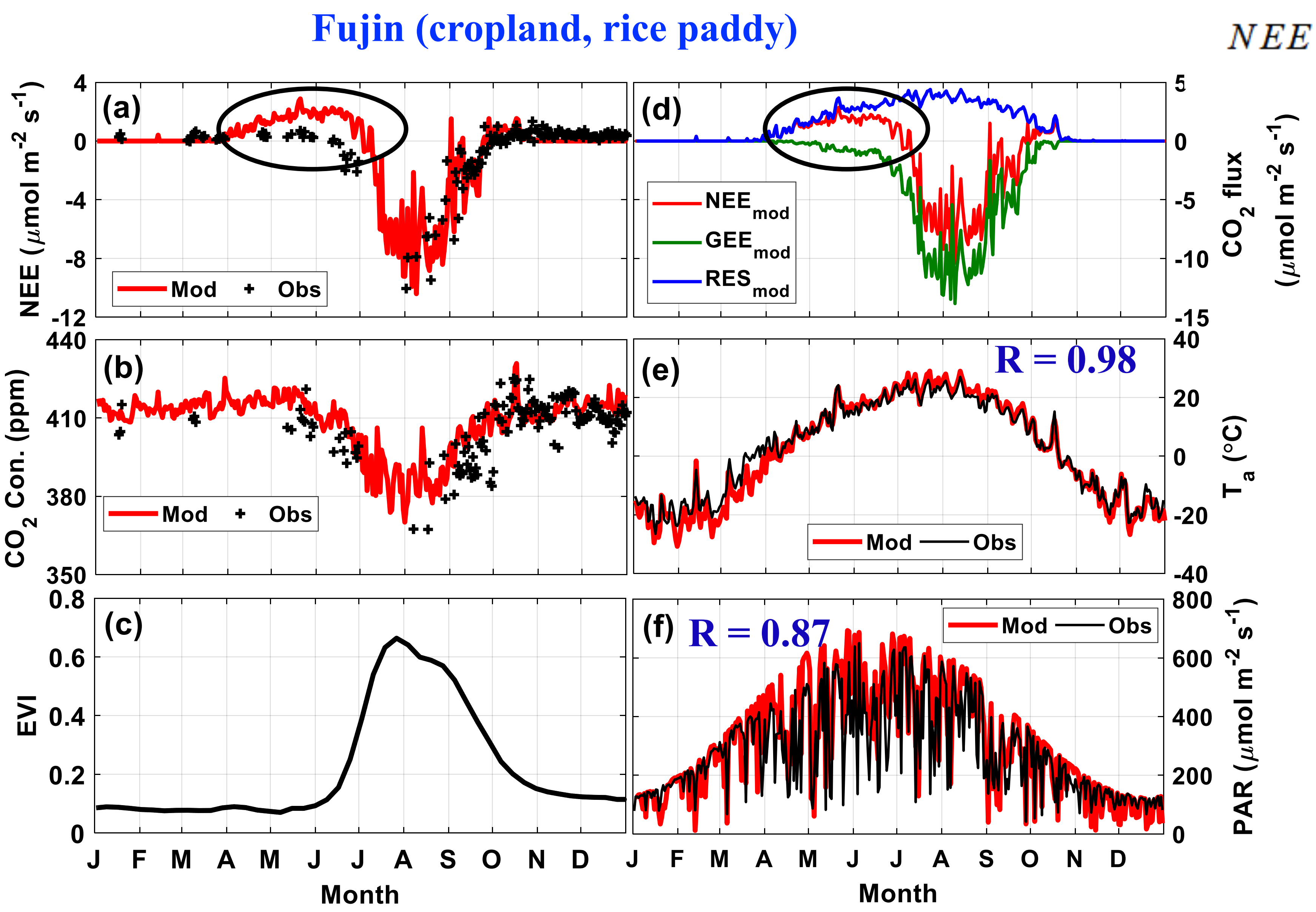

$$NEE = (\alpha \times T + \beta) + GEE$$

largely subjected to the EVI

Ignores leaf mass, involves EVI?

Seasonal variation of CO_2 fluxes and concentrations

Wuying (mixed forest)

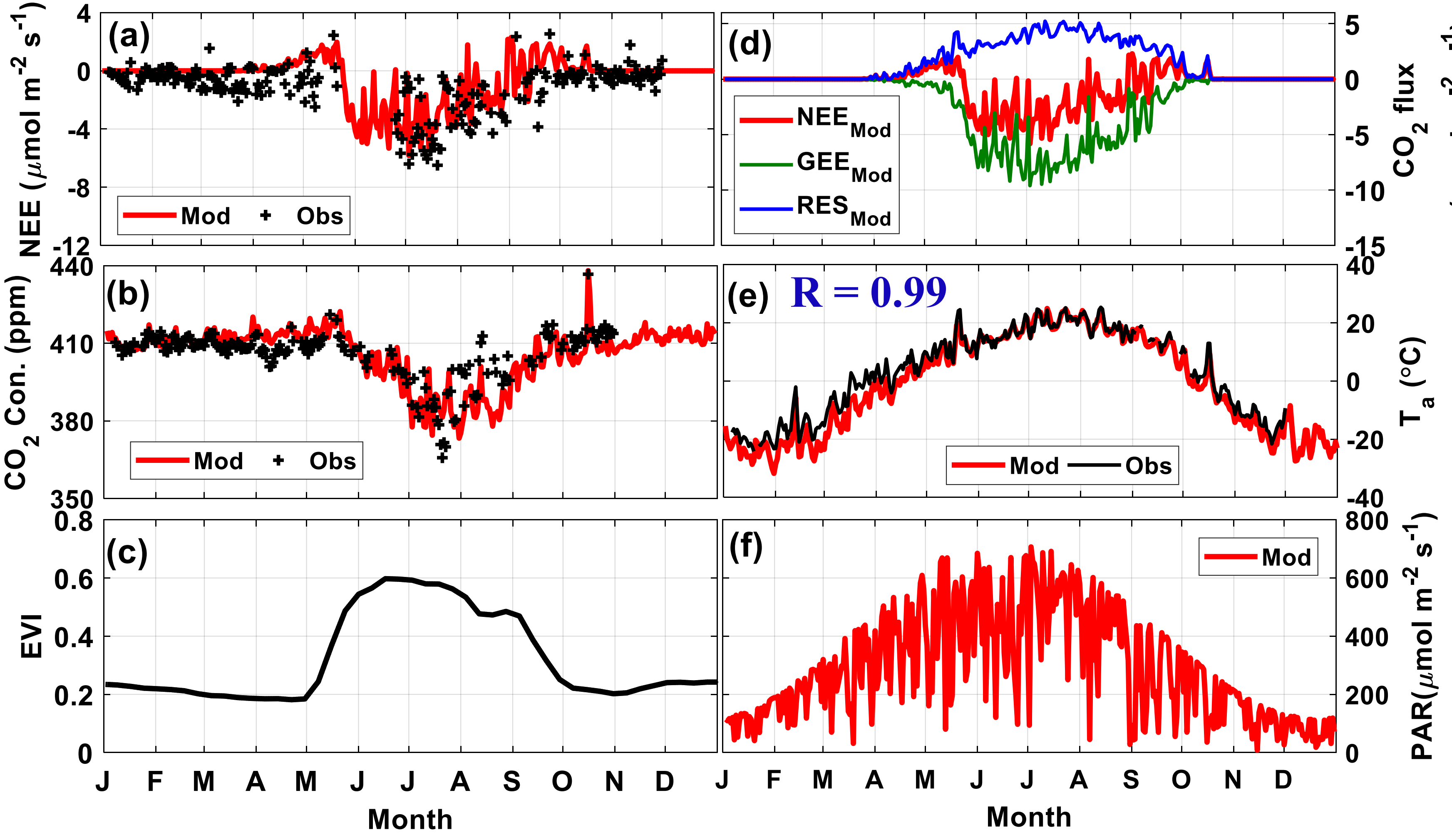

MODIS vegetation type

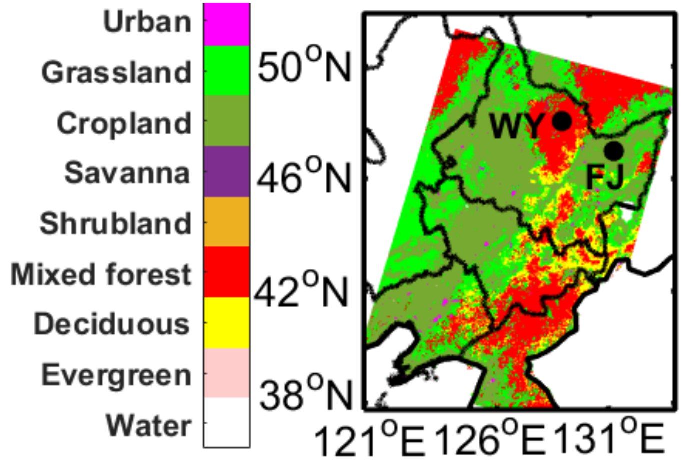

Episodic variation on October 15, 2016

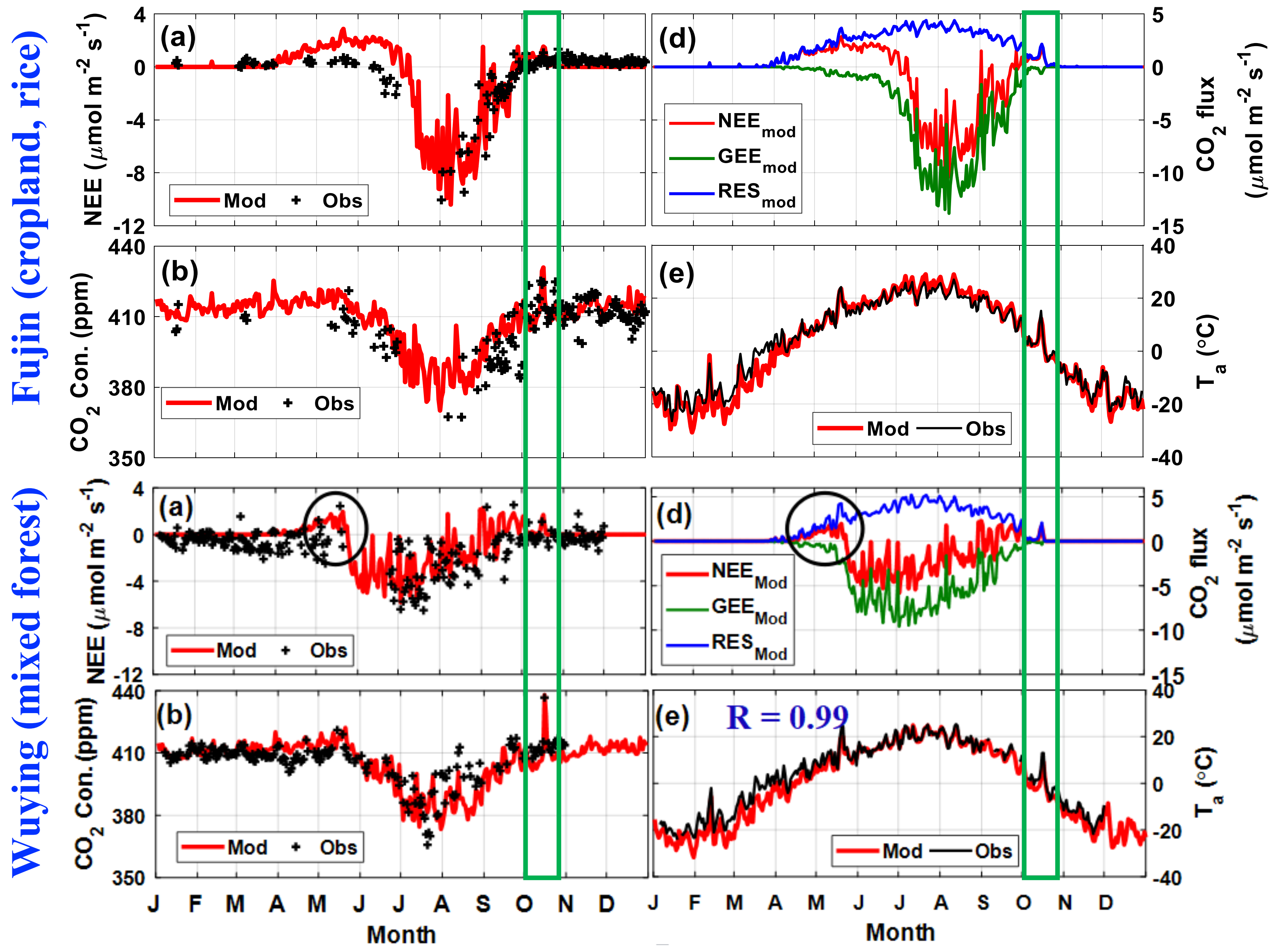

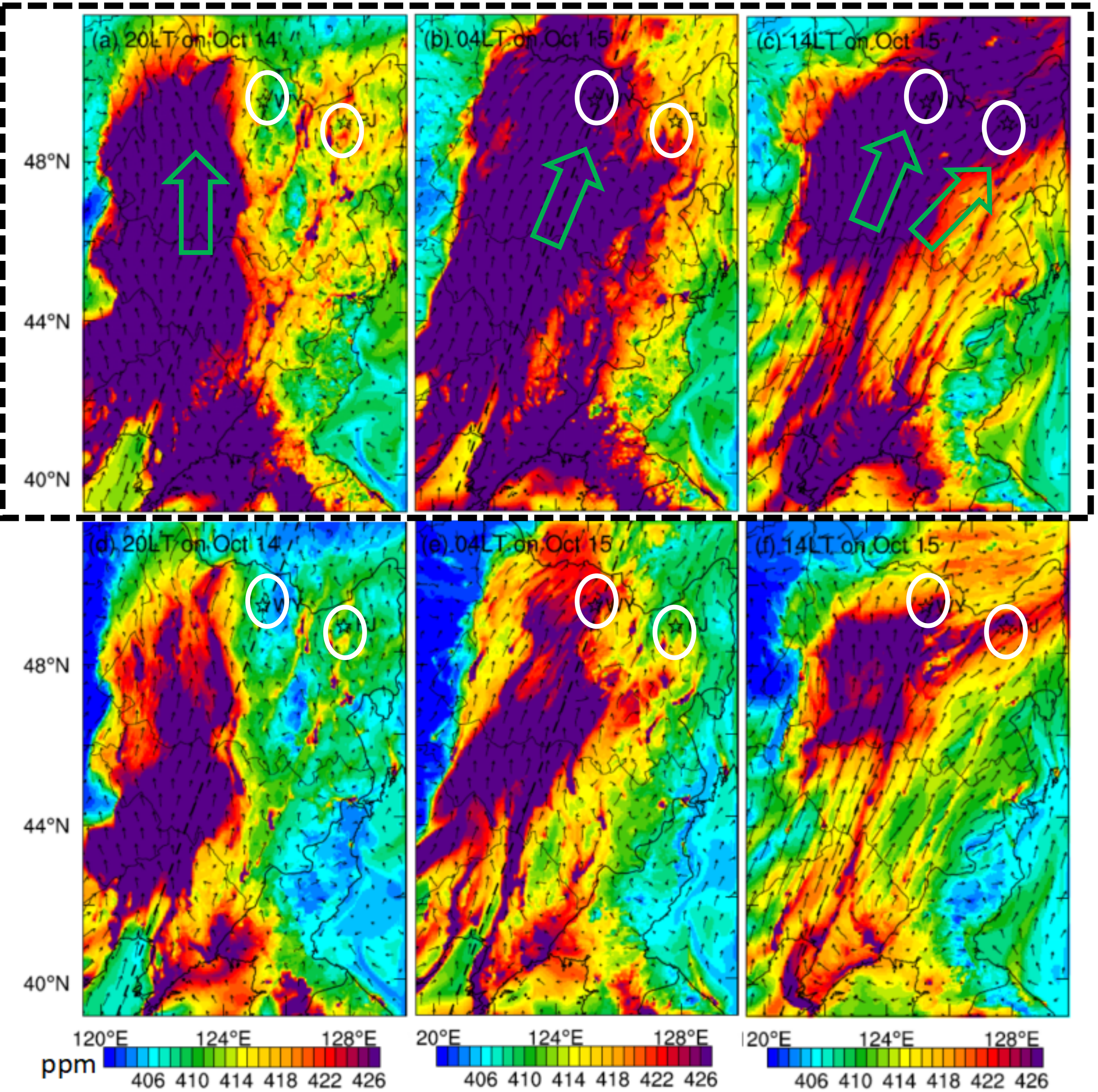

Regional transport on October 15

Anthropogenic emissions & biogenic contribution

Anthropogenic emissions only

Anthropogenic contribution: 59.4 ± 5.9%
Biogenic contribution: 40.6 ± 5.9%

Vertical cross-section on October 15

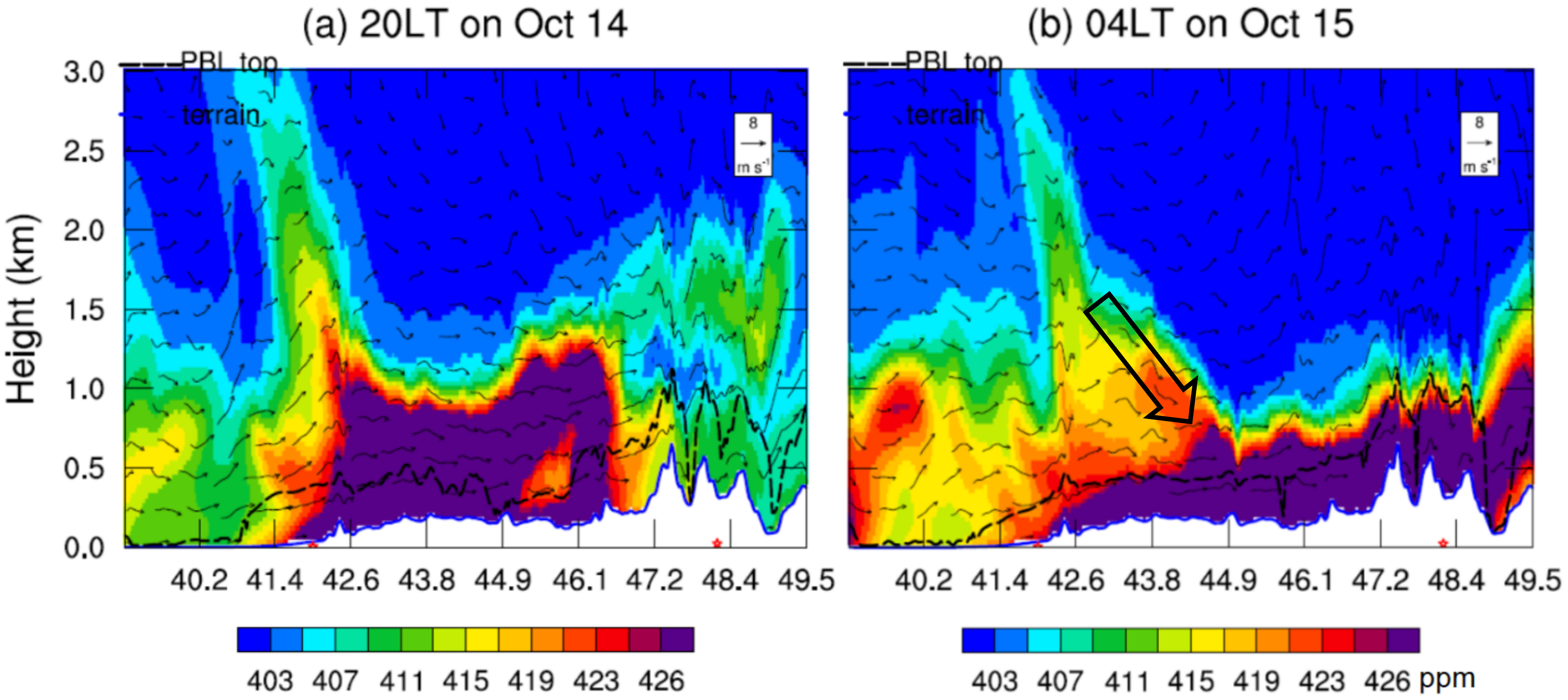

Regional transport as well as subsidence?

OCO-2 retrieved XCO_2 (L2 Lite Version 9)

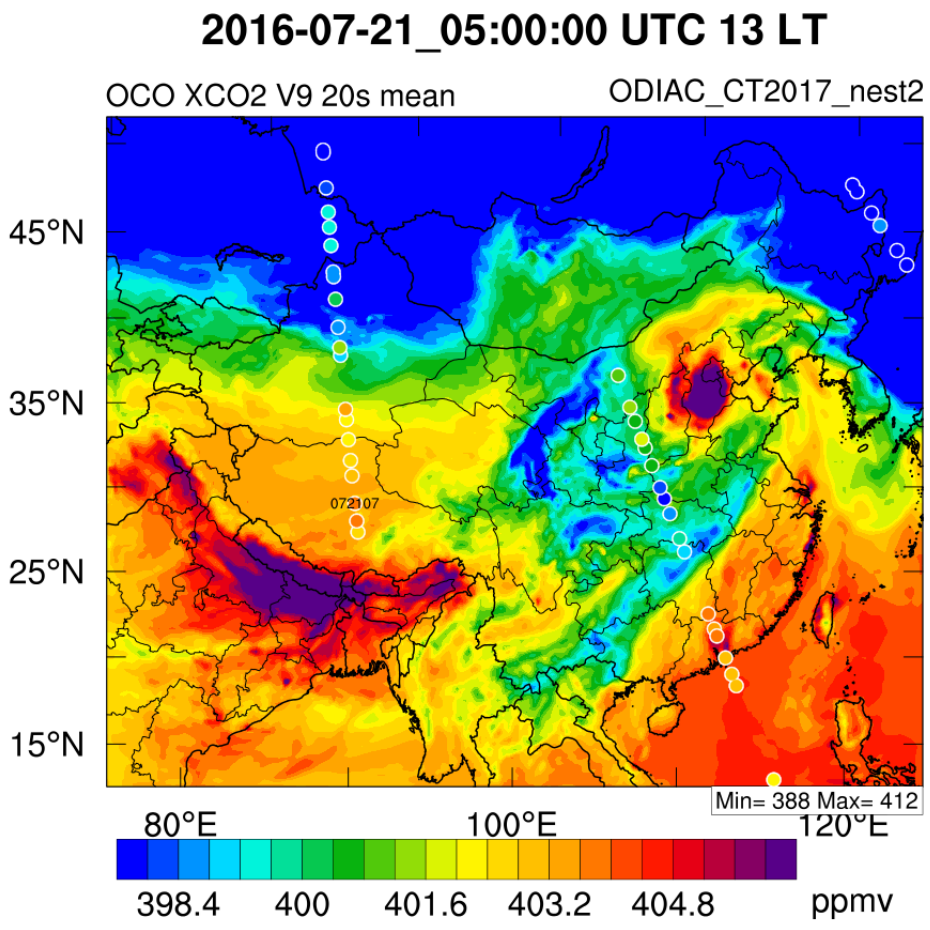

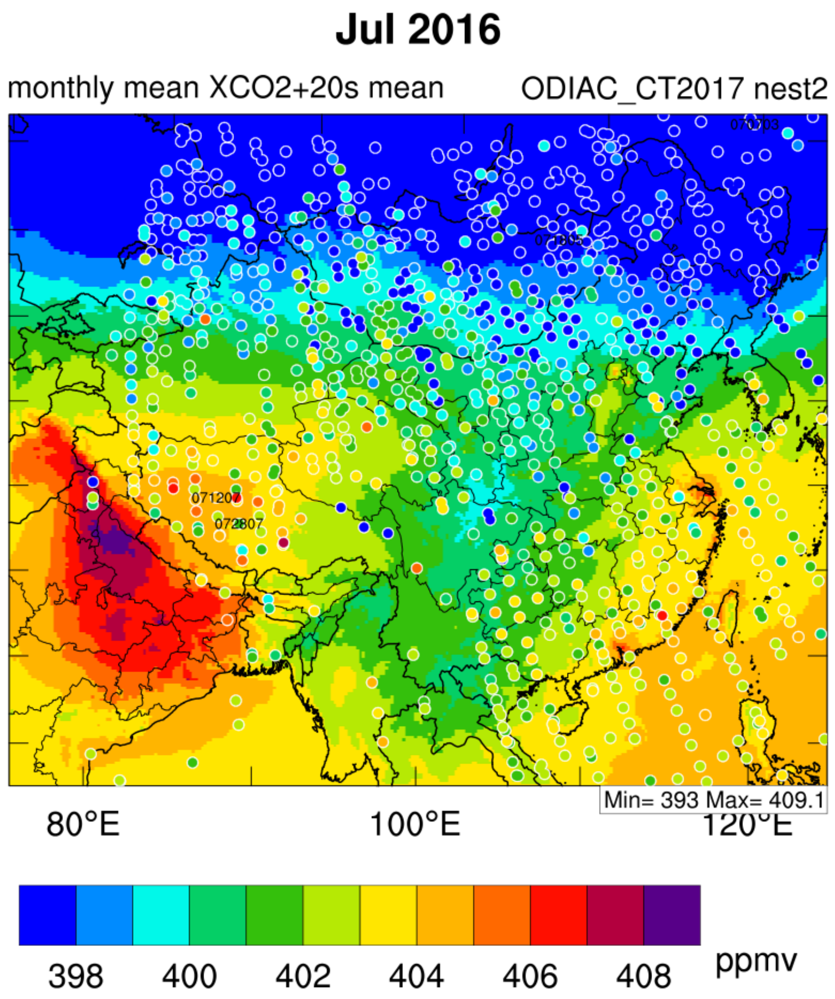

Advantage: spatiotemporal coverage

Disadvantage: interfere with cloud and haze pollution!!

Seasonal variation of XCO_2 over Northeast China

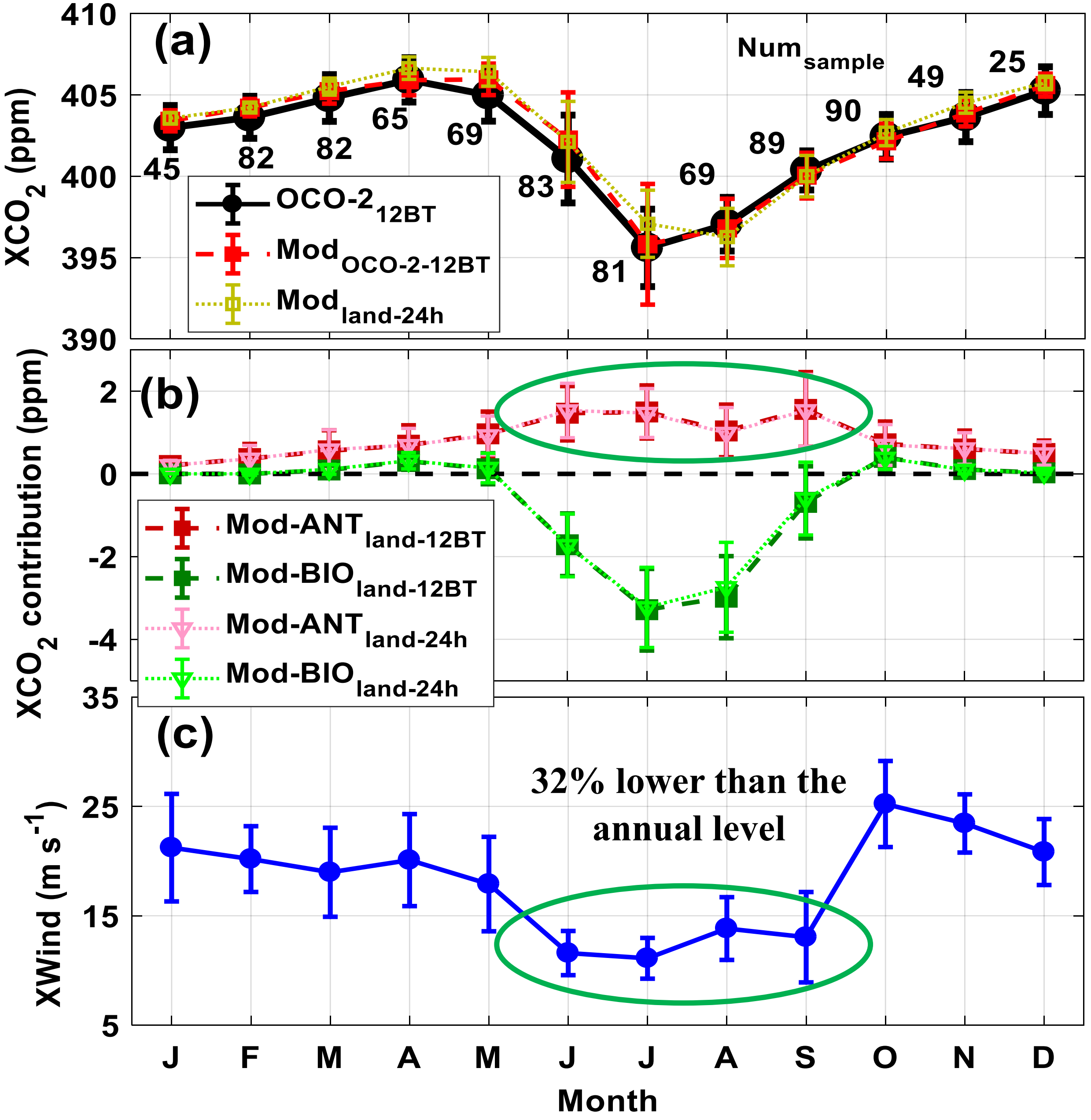

Seasonal variation range: 10 ppmv

Annual mean contribution:

- anthropogenic: 0.84 ppmv
- biogenic: -0.60 ppmv

Weak winds favors the large anthropogenic contribution of XCO_2 in summer

Mean diurnal variation of CO_2 fluxes and concentrations in growing season

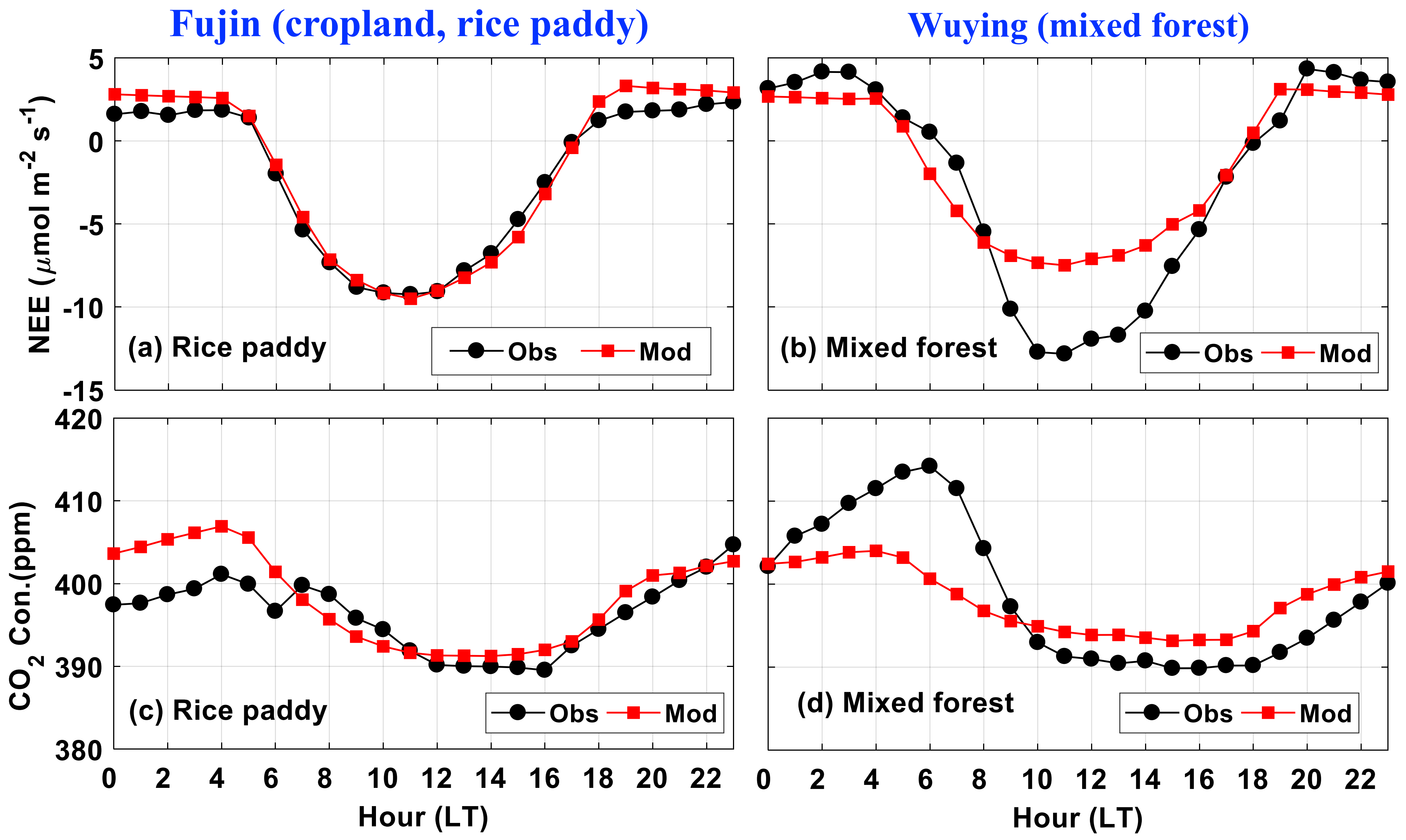

WRF-VPRM underestimates diurnal variation range over mixed forest

Ensemble offline VPRM simulations over mixed forest, predictability of CO_2 fluxes

Table 3 Range of VPRM parameters in five groups of ensemble simulations, with * representing relative variation to the default values

Ensemble Simulation	α	β	λ	PAR_0
ES1	[0.12, 0.30]	[0.50, 1.20]	[0.09, 0.14]	[350, 600]
	-40 ~ 50%*	-50 ~ 20%*	-10 ~ 40%*	-16.57 ~ 43.03%*
ES2	[0.12, 0.30]	1	0.1	419.5
ES3	0.2	[0.50, 1.20]	0.1	419.5
ES4	0.2	1	[0.09, 0.14]	419.5
ES5	0.2	1	0.1	[350, 600]

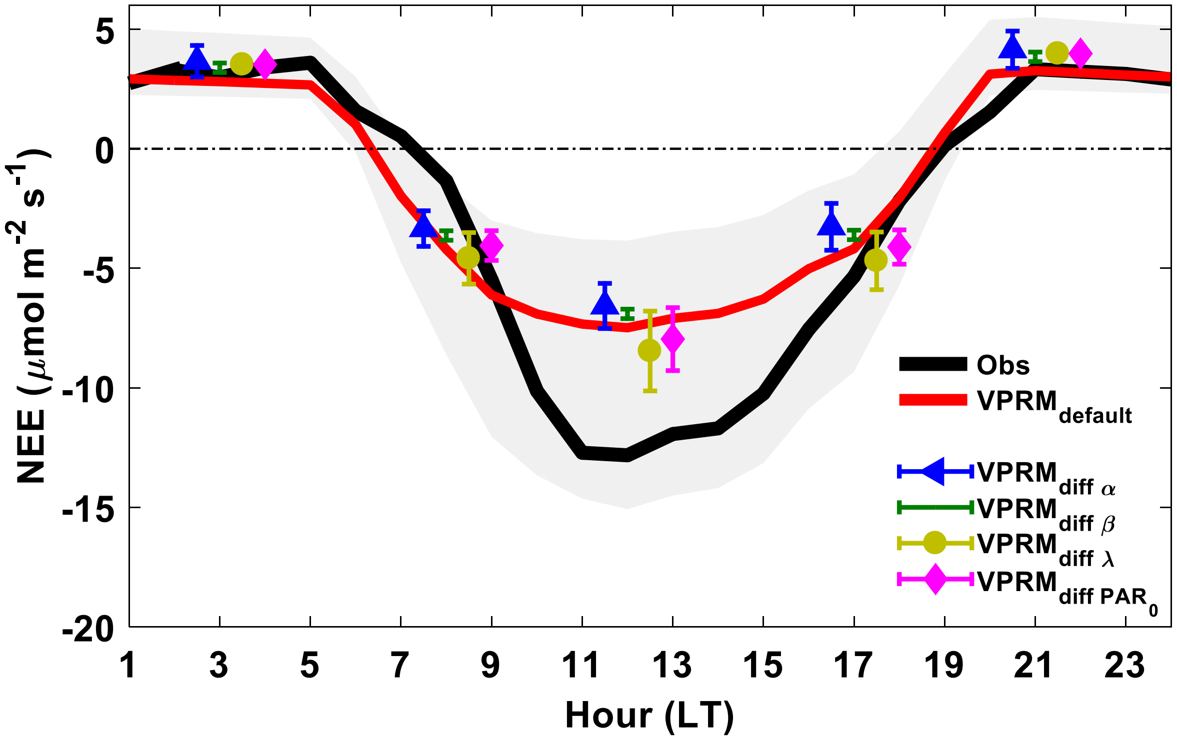

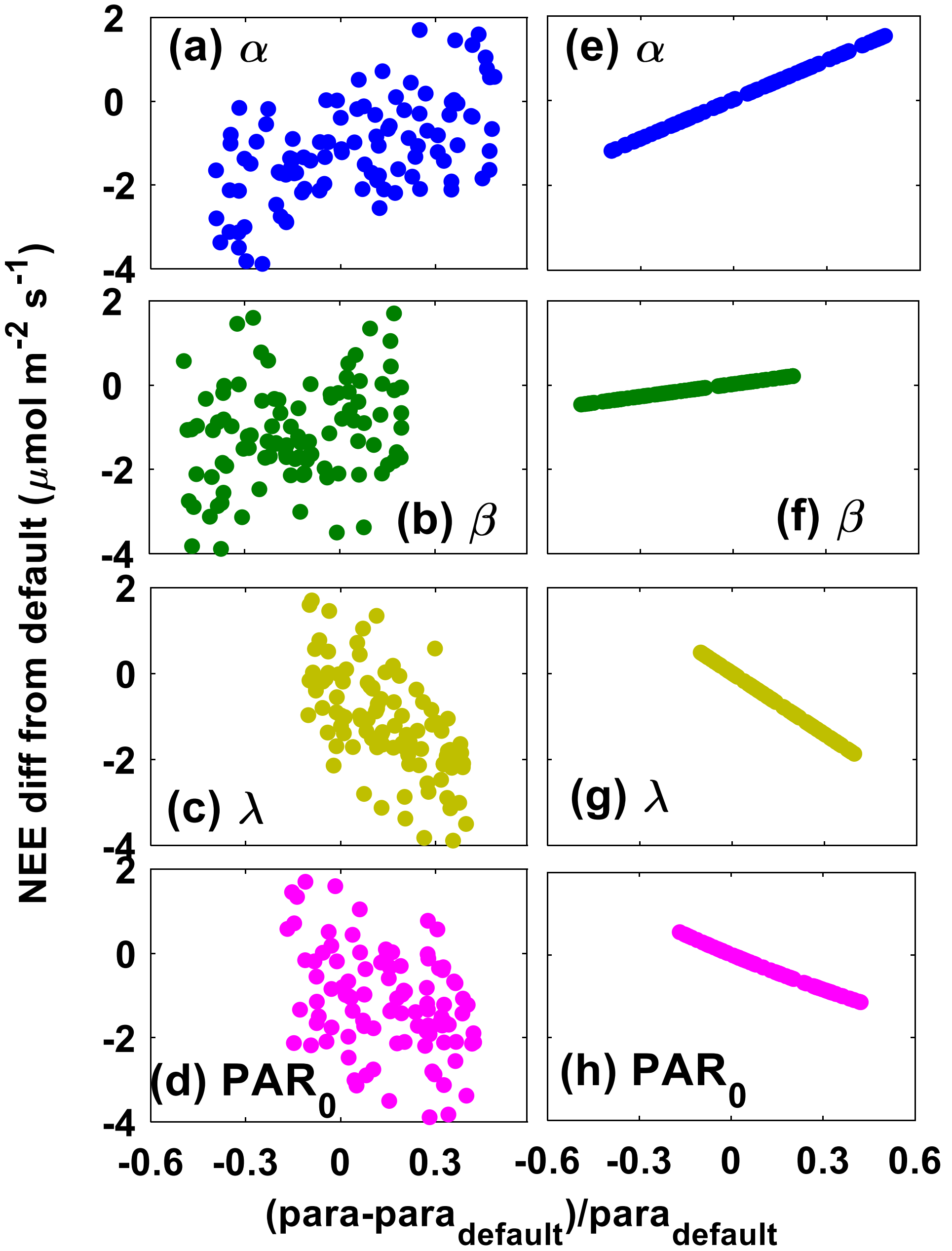

Conclusions and future work

- **Mixed forest is observed as a stronger CO_2 sink/source than rice paddy on average in 2016;**
- **Negative biogenic contribution offset about 70% of anthropogenic contribution of XCO_2 over Northeast China in 2016;**
- **The uncertainty of NEE simulation largely depends on four VPRM parameters, especially the maximum light use efficiency λ.**

Future: Update VPRM in WRF, including update the GEE equation and parameters.

$$GEE = (\lambda \times T_{scale} \times W_{scale} \times \cancel{P_{scale}}) \times FAPAR_{PAV} \times 1/(1+PAR/PAR_0) \times PAR$$

$$FAPAR_{PAV} = \cancel{EVI}$$

1.25*(EVI-0.1)

Also separate crop into C3/C4

CO_2 models

- Global models:
  - －Chemistry transport model TM3 (Heiman, 1996), TM5 (Krol et al., 2005)
  - －Laboratoire de Met´ eorologie Dynamique, LMDZ（Hauglustaine et al., 2004）
  - －ECHAM-4 (Max Planck Institute for Meteorology)
  - －CarbonTracker (only simulate CO_2 fluxes, not CO_2 concentrations)

- Regional models:
  - －NCAR episodic regional chemical transport mode, HANK（Hess et al., 2000）
  - －Danish Eulerian Hemispheric Model, DEHM (Christensen, 1997)
  - －REgional MOdel, REMO(Majewski, 1991)
  - －DEHM-LSM (land surface model), (Geel et al., 2004)
  - －RAMS-SiB2(Scott Denning et al., 2003)

Reference: https://www.atmos-chem-phys.net/7/3461/2007/acp-7-3461-2007.pdf